UNITED NATIONS EDUCATIONAL, SCIENTIFIC AND CULTURAL ORGANIZATION
INTERNATIONAL ATOMIC ENERGY AGENCY
INTERNATIONAL CENTRE FOR THEORETICAL PHYSICS
I.C.T.P., P.O. BOX 586, 34100 TRIESTE, ITALY, CABLE: CENTRATOM TRIESTE

SMR.998b - 6

Research Workshop on Condensed Matter Physics
30 June - 22 August 1997
MINIWORKSHOP ON
SUPERCONDUCTING MESOSCOPIC STRUCTURES

14 - 25 JULY 1997

"Subgap current in mesoscopic superconducting junctions"

V. SHUMEIKO
Chamers University of Technology
Microelectron and Nanoscience
Rannvagen 6
S-41296 Gothenburg
SWEDEN

These are preliminary lecture notes, intended only for distribution to participants.

Scattering theory of superconductive tunneling in quantum junctions

V. S. Shumeiko[1,2] and E. N. Bratus,[1,2]

[1]*Department of Applied Physics, Chalmers University of Technology and Göteborg University, S-41296 Göteborg, Sweden and* [2]*B. Verkin Institute for Low Temperature Physics and Engineering, 47 Lenin Ave., 310164 Kharkov, Ukraine*

G. Wendin[1]

Department of Applied Physics, Chalmers University of Technology and Göteborg University, S-41296 Göteborg, Sweden

(Submitted September 11, 1996; revised September 27, 1996)
Fiz. Nizk. Temp. **23**, 249–270 (March 1993)

A consistent theory of superconductive tunneling in single-mode junctions within a scattering formulation of Bogolyubov-de Gennes quantum mechanics is presented. The dc Josephson effect and the dc quasiparticle transport in the voltage-biased junctions are considered. Elastic quasiparticle scattering by the junction determines the equilibrium Josephson current. The origin of Andreev bound states in tunnel junctions and their role in equilibrium Josephson transport are discussed. In contrast, quasiparticle tunneling in voltage-biased junctions is determined by inelastic scattering. A general expression for inelastic scattering amplitudes is derived and the quasiparticle current is calculated at all voltages with emphasis on a discussion of the properties of subgap tunnel current and the nature of subharmonic gap structure.
 [S1063-777X(97)00203-X]

1. INTRODUCTION

The tunnel Hamiltonian model[1] has for many years been a main theoretical tool for investigation of tunneling phenomena in superconductors.[2] However, interpretation of recent experiments on transmissive tunnel junctions[3–5] and complex superconductor-semiconductor structures[6,7] requires more detailed knowledge of the mechanisms of the superconductive tunneling than the tunnel model is able to provide. Particularly informative are experiments on superconducting quantum point contacts with controlled number of transport modes and transparency, such as controllable superconducting break junctions[8] and gate-controlled superconductor-semiconductor devices.[9] Since only a few transport modes with controlled transparency are involved in the tunnel transport; the experiments provide precise and detailed information which can be directly compared with theory.

The first attempts to develop a theory of superconductive tunneling beyond the tunnel Hamiltonian model[10–13] were made in generalization of methods applied to *SNS* junctions[14,15] and superconducting constrictions[16,17] based on the Green's function methods. In these theories, the junction Green's functions are directly found from the Green's function equations which are supplemented by special boundary conditions representing the tunnel barrier or by matching the superconductor and insulator Green's functions at the superconductor-insulator boundaries.

In the first studies of the Josephson effect in *SNS* junctions[18,19] another method of calculation, based on expansion over eigenstates of the Bogolyubov-de Gennes (BdG) equation, has been used.[20] A similar method has been also applied to *SIS* tunnel junctions[21] and superconductor-semiconductor junctions.[22] In the absence of inelastic scattering the method of using the BdG equation gives the same results as the Green's function method.[21] One might then expect that the Josephson effects in superconducting junctions can be explained on a rather simple quantum-mechanical level. Following this idea, the quantum-mechanical approach has been successfully applied to calculation of the direct Josephson current in different kinds of mesoscopic weak links[24–28] and tunnel junctions.[29–31] This method was applied for the first time to voltage-biased junctions by Blonder, Tinkham, and Klapwijk, who considered quasiparticle tunneling in *SIN* junctions as a scattering problem in BdG quantum mechanics.[23] Later, the quantum-mechanical approach has been found helpful in investigations of more complex phenomena of quasiparticle transport and ac Josephson effect in voltage-biased *SNS* junctions,[32] mesoscopic *SIS* tunnel junctions[33] and mesoscopic constrictions.[34]

The quantum-mechanical approach based on the BdG equation is adequate for describing the physical situation in mesoscopic junctions, where the inelastic scattering effects are weak and most important is the coherent electron dynamics. Because of the quantization of transverse electron modes in mesoscopic junctions,[24,35] 1*D* models for the current transport through the junction may be appropriate.

In this paper we present a consistent quantum-mechanical theory of superconductive tunneling in a one-mode quantum constriction (Fig. 1). We consider the dc Josephson effect and also dc quasiparticle tunneling in the voltage-biased junctions. In the latter case we focus attention

 1063-777X/97/030181-18$10.00

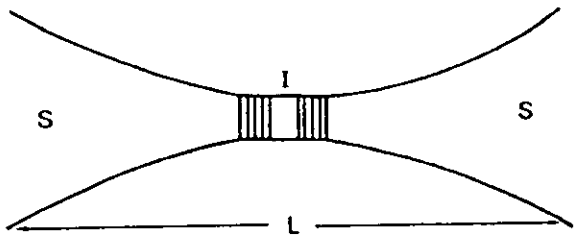

FIG. 1. *SIS* tunnel constriction.

on a detailed calculation of the subharmonic gap structure (SGS) of the tunnel current.[33]

Following the Landauer approach,[36] we consider superconducting electrodes as equilibrium reservoirs which emit quasiparticles into the constriction. Scattering by the junction goes into two channels; (i) the normal channel in which the outgoing quasiparticles remain in the same branch of the quasiparticle spectrum, and (ii) the Andreev channel in which quasiparticles change branch due to electron-hole conversions. The current in such a picture results from the imbalance of currents carried by scattering states originating from the left and the right reservoirs. Here the magnitude of the current is proportional to the transmission coefficient D of the tunnel barrier.

The imbalance of currents in superconducting junctions can be created in two ways: by establishing a difference in the phases of the order parameters in the left and right electrodes or by applying a voltage bias. The basic fact concerning the flow of equilibrium current in the presence of a phase difference, which was established by Furusaki and Tsukada,[29] is that a bulk supercurrent is, upon approaching the tunnel interface, transformed into a current that flows through the superconducting bound states which appear at the tunnel interface in the presence of the phase difference[37] and which provide transmission of the Cooper pairs through the tunnel barrier. The balance among currents of different scattering states is not violated, although the scattering amplitudes depend strongly on the phase difference.

Application of a voltage bias gives rise to more far-reaching consequences than just the imbalance of the elastic scattering modes: the scattering states themselves are modified in a nontrivial way. This follows from the fact that the scattering amplitudes, which are phase-dependent at equilibrium, become time-dependent in accordance with the Josephson relation,[38] $d\varphi/dt = 2eV$, when voltage is applied. Thus, in the presence of a constant voltage the superconducting junction behaves as an effective nonstationary scatterer, whose transmissivity oscillates. This property of the superconducting junctions gives rise to ac Josephson effect; however, it is also significant for dc quasiparticle transport, because the quasiparticle transmission through such a scatterer is *inelastic*.

The physical mechanism of inelastic quasiparticle transmission through voltage-biased superconducting junctions has been first considered in *SNS* junctions,[32] where it has been explained in terms of multiple Andreev reflections (MAR): the normal quasiparticles, which are confined between superconducting walls, are permanently accelerated by the static electric field due to sequential electron-hole conversions at the *NS* interfaces, similarly to acceleration of the electrons in an ordinary potential well by a time-dependent electric field. Similar arguments can be extended to the tunnel junctions.[39] However, in tunnel junctions the scattering theory approach is more appropriate because of the quantum nature of quasiparticle transmission through the atomic-size tunnel barrier. This introduces a side band spectrum of scattered waves where the side band energies are shifted with respect to the energy of the incident wave by integer number of quanta of the scatterer frequency.[33] Such an approach is familiar in the theory of quantum scattering by oscillating potential barriers in normal tunnel junctions (see, e.g., Refs. 40 and 41 and the references cited there).

The tunneling through all the inelastic channels (normal and Andreev channels) constitutes a complete picture of superconductive tunneling in biased Josephson junctions—the incoherent part of the side band currents, which correspond to the direct quasiparticle current, and the side band interference currents, which correspond to the alternating Josephson current. An important aspect of this picture is that the Andreev bound states are involved in the current transport together with the extended side band states, which give a multiparticle character to the superconductive tunneling in the subgap voltage region. This multiparticle origin of the subgap tunnel current was first pointed out by Schrieffer and Wilkins.[42]

The structure of the paper is as follows. After formulation of the problem and discussion of the quasiclassical approximation in Sec. 2, we consider the problem of elastic scattering in Sec. 3 as a starting point for construction of inelastic scattering states in biased junctions. The solution of the elastic scattering problem allows us to calculate the dc Josephson current, which is done for completeness in Sec. 4. In Sec. 5 we construct inelastic scattering states and derive a continued-fraction representation for the scattering amplitudes. In Sec. 6 we derive the nonequilibrium current. In Sec. 7 we discuss the origin of the excess tunnel current in the large bias limit. In Sec. 8 we present a general analysis of the subgap tunnel current. Finally, the *SGS* is analyzed in Sec. 9.

2. FORMULATION OF THE MODEL

We consider a superconducting quantum constriction with adiabatic geometry[43]: the cross section varies smoothly with the coordinate x on the scale of the Fermi electron wavelength $1/p_F$, and the size of the cross section is comparable with the Fermi electron wavelength (Fig. 1). The length L of the constriction is assumed to be smaller than the superconducting coherence length ξ_0:

$$1/p_F \ll L \ll \xi_0. \tag{2.1}$$

The Hamiltonian of the constriction is assumed to have the form

$$\hat{H}=\left[\frac{(\hat{p}-\sigma_z e\mathbf{A}(\mathbf{r},t))^2}{2m}+U(r)-\mu\right]\sigma_z$$

$$+[V(x)+e\varphi(\mathbf{r},t)]\sigma_z+\hat{\Delta}(\mathbf{r},t), \qquad (2.2)$$

where $U(\mathbf{r})$ is the potential which confines the electrons within the constriction; $V(x)$ is the potential of the tunnel barrier; $\mathbf{A}(\mathbf{r},t)$ and $\varphi(\mathbf{r},t)$ are electro-magnetic potentials; $\hat{\Delta}(\mathbf{r},t)$ is the off-diagonal superconducting order parameter given by the matrix

$$\hat{\Delta}=\begin{pmatrix}0 & \Delta e^{i\chi/2}\\ \Delta e^{-i\chi/2}0 & \end{pmatrix}. \qquad (2.3)$$

We assume that the junction is symmetric. The choice of the units corresponds to $c=\hbar=1$.

It is convenient to eliminate the phase of the superconducting order parameter $\chi(\mathbf{r},t)$ in Eq. (2.3) by means of a gauge transformation:

$$\exp(i\sigma_z\chi/2)\hat{H}\exp(-i\sigma_z\chi/2)\to\hat{H}, \qquad (2.4)$$

which allows us to introduce a gauge-invariant superfluid momentum, $\mathbf{p}_s=\nabla\chi/2-e\mathbf{A}$, and an electric potential $\Phi=\dot{\chi}/2+e\varphi$.

There are different scales of change of potentials in Eq. (2.2): one is an atomic scale over which the confining potential $U(r_\perp)$ and the potential of the tunnel barrier $V(x)$ change. Other scales are related to the changes in the superconducting order parameter, the electromagnetic field penetration lengths and the length of the contact: all these lengths are large in comparison with the atomic length. It is convenient to separate these two scales by introducing quasiclassical wave functions,[44] which vary slowly on an atomic scale, and by including rapidly varying potentials in a boundary condition for quasiclassical wave functions. To this end, we assume that the solution $\Psi(\mathbf{r},t)$ of the Bogolyubov-de Gennes equation[20]

$$i\dot{\Psi}(t)=\hat{H}\Psi(t), \qquad (2.5)$$

with the Hamiltonian of Eq. (2.2), has a quasiclassical form

$$\Psi(\mathbf{r},t)=\sum_\beta \psi_\perp(\mathbf{r}_\perp,x)\frac{1}{\sqrt{v}}\exp\left(i\beta\int p\,dx\right)\psi^\beta(x,t), \qquad (2.6)$$

where $\psi_\perp$ is the normalized wave function of the quantized transverse electron motion with the energy $E_\perp$,

$$\left(\frac{\hat{\mathbf{p}}_\perp^2}{2m}+V(\mathbf{r}_\perp,x)\right)\psi_\perp=E_\perp(x)\psi_\perp,$$

$$\psi_\perp(r_\perp=\infty,x)=0,$$

and p is the longitudinal momentum of the quasiclassical electron, $p(x)=[2m(\mu-E_\perp(x))]^{1/2}$; $\beta=\pm$ indicates the direction of the electron motion. We assume that the constriction has only one transport mode; an extension to the case of several unmixed modes consists of additional summation over all transport modes in the equation for the current. The coefficients ψ^β in Eq. (2.6) describe the wave functions which vary slowly in the x direction and which satisfy the reduced BdG equation

$$i\dot{\psi}^\beta_{L,R}=(\beta v\hat{p}\sigma_z+\Phi_{L,R}\sigma_z+vp_{sL,R}+\Delta\sigma_x)\psi^\beta_{L,R} \qquad (2.7)$$

in the left (L) and the right (R) electrodes; $v=p/m$. The potentials $\mathbf{p}_s$ and Φ describe the distributions of the electromagnetic field and supercurrent in the electrodes. In the point contact geometry these quantities are small due to the effect of spreading out of the current.[16,45] We will therefore omit them, $\mathbf{p}_s=\Phi=0$. For the same reason, deviation of the spatial distribution of the module of the order parameter Δ from constant value is small in the point contacts; we will therefore ignore it, $\Delta=$ const.

The functions $\psi^\beta_{L,R}$ are matched at the constriction by the boundary condition[31] (see also Appendix A):

$$\begin{pmatrix}\psi^-_L\\ \psi^+_R\end{pmatrix}=\hat{V}\begin{pmatrix}\psi^+_L\\ \psi^-_R\end{pmatrix}\quad\text{at } x=0, \qquad (2.8)$$

with a matching matrix $\hat{V}$

$$\hat{V}=\begin{pmatrix}r & de^{i\sigma_z\varphi/2}\\ de^{-i\sigma_z\varphi/2} & r\end{pmatrix}. \qquad (2.9)$$

The quantities d and r are the normal electron transmission and reflection amplitudes due to the barrier. Here and further φ is a gauge-invariant difference in the superconducting phases of the right and left electrodes: $\varphi=\chi_R(0)-\chi_L(0)$. The matching matrix in Eq. (2.9) satisfies the unitarity condition

$$\hat{V}\hat{V}^+=1. \qquad (2.10)$$

The boundary condition in Eqs. (2.8) and (2.9) is analogous to the boundary condition used in the quasiclassical Green's function methods (see, e.g., Refs. 11 and 46). This is a very simple equation for coupling of superconducting electrodes, while retaining the main features of the Josephson effect, except for effects of the resonant tunneling.[30,47,48]

3. ELASTIC SCATTERING

In the absence of time dependence in the phase difference at the junction, $\dot{\varphi}=0$, Eqs. (2.7) and (2.8) describe elastic scattering of quasi-particles. The scattering states can be constructed by using stationary solutions of Eq. (2.7), which correspond to elementary propagating waves with energy $|E|>\Delta$:

$$\psi^{\beta\alpha}_E=\exp(-iEt+i\beta\alpha(\xi/v)x)u^\delta_E, \qquad (3.1a)$$

$$u^\delta_E=(2\cosh\gamma)^{1/2}\begin{pmatrix}e^{\delta\gamma/2}\\ \sigma e^{\delta\gamma/2}\end{pmatrix}, \qquad (3.1b)$$

where

$$\xi=\sqrt{E^2-\Delta^2},\quad e^\gamma=\frac{|E|+\xi}{\Delta},$$

$$\sigma=\operatorname{sign}E,\quad \alpha=\pm,\quad\text{and}\quad \delta=\alpha\sigma. \qquad (3.2)$$

The vector function μ_E is normalized, $(u,u)=1$; the brackets mean that the scalar product is in the electron-hole space. In Eq. (3.1) there are four elementary waves, which correspond to the same energy, as illustrated in Fig. 2, and which are labeled by quantum numbers β (direction of the Fermi electron momentum) and $\alpha=\operatorname{sign}(|p|-p_F)$ (the electron or

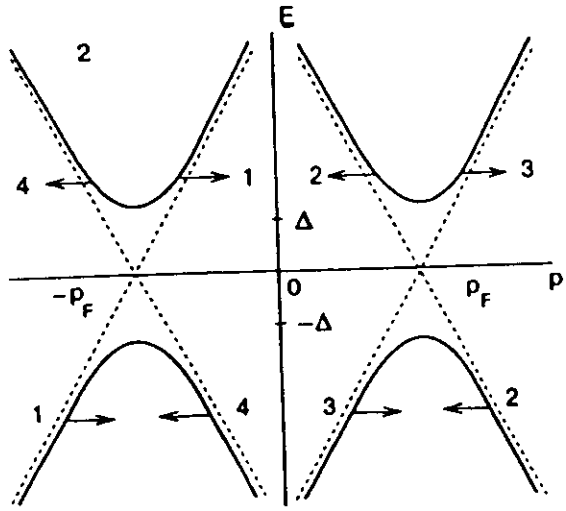

FIG. 2. Quasiparticle spectrum and position of the incoming states: 1(3)—hole (electron)-like quasiparticle incident from left; 2(4)—hole (electron)-like quasiparticle incident from right.

hole-like branch of the quasiparticle spectrum). The direction of propagation of each elementary wave is determined by the sign of the probability current. The probability current density j_p, which is defined by the conservation law (the continuity equation) $\partial|\psi|^2/\partial t+\partial j_p/\partial x=0$ for the BdG equation [Eq. (2.7)], has the form $j_p=(\psi,\sigma_z\psi)$. For the elementary waves in Eq. (3.1), we obtain the explicit result $j_p=\beta\delta\tanh\gamma$. According to this formula, the relation $\delta=\beta$ is satisfied for the waves propagating from left to right, and the relation $\delta=-\beta$ is satisfied for the waves propagating from right to left. Therefore, the incoming waves from the left (L) and the right (R) have the form

$$\text{L:}\exp(i\sigma(\xi/v)x)u_E^{\beta},\quad \text{R:}\exp(-i\sigma(\xi/v)x)u_E^{-\beta}. \tag{3.3}$$

while the outgoing waves have the form

$$\text{L:}\exp(-i\sigma(\xi/v)x)u_E^{-\beta},\quad \text{R:}\exp(i\sigma(\xi/v)x)u_E^{\beta}. \tag{3.4}$$

Correspondingly, the incoming quasiparticle can be scattered into four outgoing states: two forward-scattering states and two backscattering states. One of the reflected waves belongs to the same (electron-like or hole-like) branch of the quasiparticle spectrum as the incoming wave and constitutes the normal scattering channel, while the other reflected wave changes the spectrum branch and constitutes the Andreev channel. In a similar way, transmitted waves constitute normal and Andreev channels. The structure of the scattering states then becomes

$$\begin{pmatrix}\psi_L\\ \psi_R^+\end{pmatrix}=\begin{pmatrix}\delta_{j,1}\\ \delta_{j,2}\end{pmatrix}e^{i\sigma(\xi/v)x}u_E+\begin{pmatrix}a\\ b\end{pmatrix}_j e^{-i\sigma(\xi/v)x}u_E^+, \tag{3.5a}$$

$$\begin{pmatrix}\psi_L^+\\ \psi_R\end{pmatrix}=\begin{pmatrix}\delta_{j,3}\\ \delta_{j,4}\end{pmatrix}e^{i\sigma(\xi/v)x}u_E^+ +\begin{pmatrix}c\\ f\end{pmatrix}_j e^{-i\sigma(\xi/v)x}u_E, \tag{3.5b}$$

(for brevity we have omitted the time-dependent factors $\exp(-iEt)$). In Eqs. (3.5) the index $j=1(2)$ corresponds to a hole-like quasiparticle that comes from the left(right), while the index $j=3(4)$ corresponds to an electron-like quasiparticle that comes from the left (right). According to the structure of the matching matrix [Eq. (2.9)], the symmetry between the scattering states $j=1$ and 2 is

$$\begin{pmatrix}a\\ b\end{pmatrix}_2(\varphi)=\begin{pmatrix}b\\ a\end{pmatrix}_1(-\varphi),\quad \begin{pmatrix}c\\ f\end{pmatrix}_2(\varphi)=\begin{pmatrix}f\\ c\end{pmatrix}_1(-\varphi). \tag{3.6}$$

Analogous symmetry exists also for the scattering states $j=3,4$. Using the unitarity of the matching matrix [Eq. (2.9)], we can find the following relation between the scattering states $j=3$ and 1:

$$\begin{pmatrix}a\\ b\end{pmatrix}_3(\gamma,r,d)=\begin{pmatrix}c\\ f\end{pmatrix}_1(-\gamma,r^*,d^*),$$

$$\begin{pmatrix}c\\ f\end{pmatrix}_3(\gamma,r,d)=\begin{pmatrix}a\\ b\end{pmatrix}_1(-\gamma,r^*,d^*). \tag{3.7}$$

These symmetry relations allow us to find all the scattering amplitudes if one of the scattering states is known.

Let us find the explicit scattering amplitudes for the scattering state $j=1$. After substituting Eqs. (3.5) into Eq. (2.8), it is convenient to split the resulting equation, using the orthogonality condition, $(u^+,\sigma_z u^-)=0$, into two independent equations for the normal scattering amplitudes c,f and for the Andreev scattering amplitudes a,b:

$$(u^-,\sigma_z u^-)\begin{pmatrix}1\\ 0\end{pmatrix}=(u^-,\sigma_z\hat{V}u^-)\begin{pmatrix}c\\ f\end{pmatrix}_1, \tag{3.8a}$$

$$(u^+,\sigma_z u^+)\begin{pmatrix}a\\ b\end{pmatrix}_1=(u^+,\sigma_z\hat{V}u^-)\begin{pmatrix}c\\ f\end{pmatrix}_1. \tag{3.8b}$$

Calculating the scalar products in Eqs. (3.8), we find the explicit expression for the Andreev amplitudes in terms of the normal amplitudes,

$$\begin{pmatrix}a\\ b\end{pmatrix}_1=\frac{id\sin(\varphi/2)}{\sinh\gamma}\begin{pmatrix}f\\ -c\end{pmatrix}_1. \tag{3.9}$$

The solution of the first equation in Eq. (3.8) is given by

$$c_1=\frac{r\sinh^2\gamma}{Z},\quad f_1=-\frac{d\sinh\gamma\sinh(\gamma+i\varphi/2)}{Z}, \tag{3.10}$$

where

$$Z=-\frac{d}{d^*}(R\sinh^2\gamma+D\sinh(\gamma+i\varphi/2)$$
$$\times\sinh(\gamma-i\varphi/2)), \tag{3.11}$$

$D=|d|^2$ is the normal electron transmission coefficient of the tunnel junction, and $R=|r|^2=1-D$ is the normal electron reflection coefficient. It follows from Eqs. (3.9) and (3.10) that if there is no phase difference across the junction, $\varphi=0$, the Andreev scattering channel is closed: $a=b=0$. It is worth mentioning that the Andreev reflection is also absent if the normal transparency of the junction is equal to zero, $D=0$. If, on the other hand, the junction is completely transparent for normal electrons, $D=1$, there is no Andreev forward scattering, $b=c=0$.

In the presence of a phase difference at the junction the quasiparticle scattering is accompanied by the appearance of

superconducting bound states.[37] One can establish the existence of bound states by investigating the poles of the scattering amplitudes, Eq. (3.10), at imaginary γ corresponding to energies lying inside the gap $|E|<\Delta$. Assuming $\gamma \to i\gamma$ in Eq. (3.11), we have the dispersion equation $Z(i\gamma)=0$ or

$$\sin^2 \gamma = D \sin^2 \varphi/2. \tag{3.12}$$

The bound states correspond to a positive value of $\sin \gamma$: $\Delta \sin \gamma = \mathrm{Im}\, \xi > 0$. This condition has two roots:

$$\gamma = \gamma_0 = \arccos(\sqrt{D} \sin \varphi/2), \quad \gamma = \pi - \gamma_0 \tag{3.13}$$

or

$$E(\varphi) = \pm \Delta \sqrt{1 - D \sin^2 \varphi/2}. \tag{3.14}$$

The wave functions of the bound states can be constructed from elementary solutions of Eq. (2.7) with $|E|<\Delta$, which decay at $x = \pm\infty$:

$$\varphi^{\beta}_{E,R} = \exp(-iEt - \zeta x/v) u^{\nu}_{E}, \tag{3.15a}$$

$$\varphi^{\beta}_{E,L} = \exp(-iEt + \zeta x/v) u^{-\nu}_{E}, \tag{3.15b}$$

where

$$u^{\nu}_{E} = \frac{1}{\sqrt{2}} \begin{pmatrix} e^{i\nu\gamma/2} \\ \sigma e^{-i\nu\gamma/2} \end{pmatrix},$$

$$e^{i\gamma} = \frac{|E| + i\zeta}{\Delta}, \quad \zeta = \sqrt{\Delta^2 - E^2}, \quad \nu = \beta\sigma. \tag{3.16}$$

The bound state ansatz has a form similar to the outgoing part of the scattering states [Eq. (3.5)] with the coefficients satisfying the homogeneous equations in (3.8). These coefficients are

$$f = -\frac{d \sin(\gamma + \varphi/2)}{r \sin \gamma} c, \tag{3.17a}$$

$$\begin{pmatrix} a \\ b \end{pmatrix} = \frac{d \sin(\varphi/2)}{\sin \gamma} \begin{pmatrix} f \\ -c \end{pmatrix}, \tag{3.17b}$$

where γ is given by Eq. (3.12). We note that the bound state spectrum is nondegenerate. The coefficient c in Eqs. (3.17) is obtained from the normalization condition for the bound state wave function,

$$\int d^2 r_{\perp} \int_{x} dx |\Psi|^2 = \frac{1}{\zeta} (|a|^2 + |b|^2 + |c|^2 + |f|^2) = 1,$$

which yields

$$|c|^2 = \Delta \sin \gamma \left(1 + \frac{D}{R} \frac{\sin^2(\gamma + \varphi/2)}{\sin^2 \gamma} \right)^{-1}. \tag{3.18}$$

What is the origin of the bound states in a tunnel junction? According to Eq. (3.8), one can regard these states as resulting from hybridization of the bound states in the short ballistic constriction[24] due to the normal electron reflection by the barrier (cf. effect of impurities in the *SNS* junction[25,26]). Let us consider a smooth constriction with the length exceeding the coherence length, $L \gg \xi_0$. In such a constriction the supercurrent density and the superfluid momentum are related by the local equation, $J_s(x) = (e/m) N_s p_s(x)$, and they are both enhanced in the neck of the constriction due to current concentration (for simplicity we disregard the effect of suppression of the superfluid electron density N_s by the supercurrent). The local quasiparticle spectrum in the presence of supercurrent has an additional contribution $\pm v_F p_s(x)$,[20] which gives rise to a shift of the local energy gap (Fig. 3). The spatial bending of the gap edges forms the potential wells at $E<0 (E>0)$ for quasiparticles with electron velocities directed along (opposite) the current. The bound states in these potential wells are similar to the Andreev bound states in the *SNS* junctions.[49] The difference is that here the bound states are caused by the spatial inhomogeneity of the *phase* of the order parameter, while the original Andreev states are caused by the spatial inhomogeneity of the modulus of the order parameter. With decreasing length of the constriction, the number of the bound states in the well decreases. The short Josephson constriction corresponds to an infinitely narrow and deep δ-potential well which contains only one Andreev level.[24]

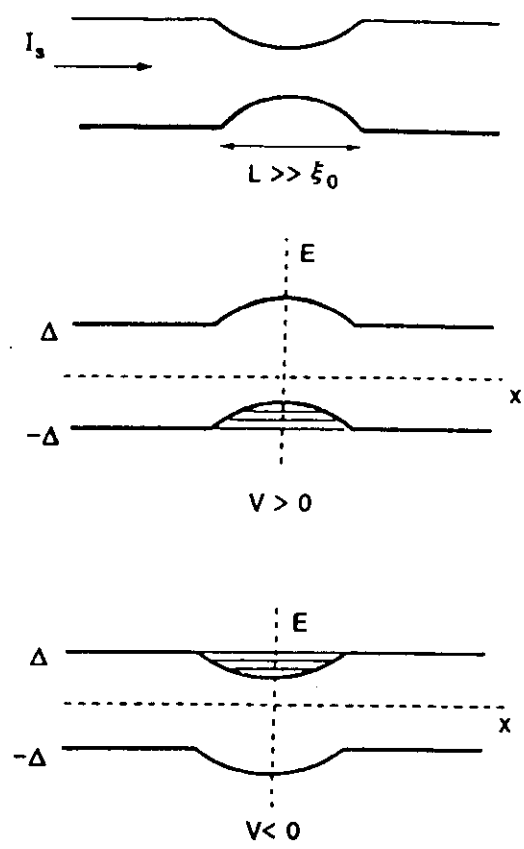

FIG. 3. Spatial configuration of the edges of the superconducting energy bands in a long constriction: $E_{\min}, E_{\max} = \pm\Delta + p_s(x)v$. A potential well appears in upper (lower) band for electrons moving in a direction opposite to (along) the supercurrent.

4. DIRECT JOSEPHSON CURRENT

A convenient expression for the tunnel current results from statistical averaging of the current operator written in the Nambu representation[50]:

$$I(x,t)=\frac{e}{2m}\left\{(\hat{p}-\hat{p}')\int d^2r_\perp \times[\delta(\mathbf{r}-\mathbf{r}')\mathrm{Tr}\langle\hat{\Psi}(\mathbf{r},t)\hat{\Psi}^+(\mathbf{r}',t)\rangle]\right\}_{\mathbf{r}=\mathbf{r}'}, \quad (4.1)$$

where $\hat{\Psi}$ is a two-component field operator

$$\hat{\Psi}(\mathbf{r},t)=\begin{pmatrix}\hat{\psi}_\uparrow(\mathbf{r},t)\\ \hat{\psi}_\downarrow^+(\mathbf{r},t)\end{pmatrix}, \quad (4.2)$$

and Tr is a trace in electron-hole space. The angular brackets in Eq. (4.1) denote a thermal average of the one-particle density matrix of the superconductor.[51] At equilibrium this matrix has the form

$$\langle\hat{\Psi}(\mathbf{r})\hat{\Psi}^+(\mathbf{r})\rangle=\sum_\lambda \Psi_\lambda(\mathbf{r})n_F(-E_\lambda)\Psi_\lambda^+(\mathbf{r}'), \quad (4.3)$$

where $\Psi_\lambda(\mathbf{r})$ are the eigenstates of the steady-state BdG equation [Eq. (2.5)] with the quantum numbers λ. We note that the definition of Fermi distribution function n_F here corresponds to the distribution of holes in the normal metal: in the ground state all energy levels above the Fermi level ($E>0$) are occupied, while energy levels below the Fermi level ($E<0$) are empty (see also the discussion in the next section). In the quasiclassical approximation [Eq. (2.6)] the average tunnel current calculated at the middle of the junction has the form

$$I=-e\sum_\lambda n_F(-E_\lambda)\sum_\beta \beta|\psi_\lambda^\beta(0)|^2. \quad (4.4)$$

The current in Eq. (4.4) can be calculated either at the left or the right side of the junction, because the equality

$$|\psi_L^+|^2-|\psi_L^-|^2=|\psi_R^+|^2-|\psi_R^-|^2, \quad (4.5)$$

due to the unitarity of the matching matrix $\hat{V}$ in Eq. (2.10), holds for each eigenstate. The current in Eq. (4.4) consists of contributions from the scattering states and the bound states:

$$I=-\int_{|E|>\Delta}\frac{dE|E|}{2\pi\xi}n_F(-E)\sum_j I_j(E)-\sum_{|E|<\Delta} n_F \times(-E)I_{\mathrm{bound}}(E),\ I(E) =e\sum_\beta \beta|\psi^\beta(E)|^2. \quad (4.6)$$

When calculating the contribution from the scattering states, it is convenient to consider the transmitted current of each scattering mode:

$$I_j(E)=\begin{cases}e(|b_j|^2-|f_j|^2) & j=1,3,\\ e(|c_j|^2-|a_j|^2) & j=2,4.\end{cases} \quad (4.7)$$

The symmetry relations [Eqs. (3.6) and (3.7)] yield

$$I_1(E)=I_4(E),\ I_2(E)=I_3(E),\ I_2(E)=-I_1(E). \quad (4.8)$$

The currents of all the scattering states with a given energy therefore cancel each other at equilibrium.[52] Substituting Eqs. (3.17) and (3.18) into Eq. (4.6), for, e.g., the right electrode, we obtain the following expression for the current of the bound state:

$$I_{\mathrm{bound}}(E)=e(|b|^2-|f|^2)=-\frac{e\Delta^2}{2E}D\sin\varphi. \quad (4.9)$$

A useful formula for the current of the single bound state, which allows direct evaluation of the current from the bound state spectrum, is given by equation

$$I(E)=2e\frac{dE(\varphi)}{d\varphi}, \quad (4.10)$$

where $E(\varphi)$ is the bound state energy band [Eq. (3.14)]. This formula is derived in Appendix B. Taking into account Eqs. (4.9) and (4.6), we write the total current in the form[10-12,53]

$$I=\frac{e\Delta D\sin\varphi}{2\sqrt{1-D\sin^2(\varphi/2)}}\tanh\frac{\Delta\sqrt{1-D\sin^2(\varphi/2)}}{2T}. \quad (4.11)$$

Thus, the Josephson direct current in tunnel junctions is carried only by the bound states, which is similar to the situation found in the other kinds of short weak links.[24-26,28,30] It follows from Eqs. (4.6) and (4.9) that the nonvanishing total current results from the imbalance of the bound state currents due to a difference in the equilibrium population numbers. Creation of a nonequilibrium population makes it possible to control the Josephson transport.[28,31,48]

5. INELASTIC SCATTERING

Let us now discuss inelastic scattering in voltage-biased junctions. According to our assumption $\Phi=0$, which is explained in Sec. 2, the applied voltage drop V is confined to the constriction; in order not to complicate the problem, we have also disregarded a small time-dependent voltage induced across the junction by the ac Josephson current (self-coupling effect[54]). This implies the following dependence on time of the phase difference:

$$\varphi=\varphi_0+2eVt. \quad (5.1)$$

The appearance of factors with periodic time dependence in the boundary condition [Eqs. (2.8) and (2.9)] gives rise to a more complex structure of the scattering states than in Eq. (3.5). In order to satisfy the boundary condition, the outgoing part of the scattering states in Eq. (3.5) is to be constructed from the eigenstates of Eq. (2.7) with different energies $E_n=E-neV$ shifted with respect to the energy E of the incoming wave with an integer $-\infty<n<\infty$ (side band structure)

$$\begin{pmatrix}\psi_L^-\\ \psi_R^+\end{pmatrix}(0)=\begin{pmatrix}\delta_{j,1}\\ \delta_{j,2}\end{pmatrix}u_E^-e^{-iEt}+\sum_n\begin{pmatrix}a\\ b\end{pmatrix}_{j,n}u_{E_n}^+e^{-iE_nt}, \quad (5.2a)$$

$$\begin{pmatrix}\psi_L^+\\ \psi_R^-\end{pmatrix}(0)=\begin{pmatrix}\delta_{j,3}\\ \delta_{j,4}\end{pmatrix}u_E^+e^{-iEt}+\sum_n\begin{pmatrix}c\\ f\end{pmatrix}_{j,n}u_{E_n}^-e^{-iE_nt}. \quad (5.2b)$$

For brevity we use the notation $u_n=u_{E_n}$. While the incoming state is itinerant, the outgoing states can be either itinerant

[Eq. (3.1) if $|E_n| > \Delta$] or bound [Eq. (3.16) if $|E_n| < \Delta$]. It is convenient to combine the two equations for the functions u_n in a single analytical form:

$$u_n^{\pm} = \frac{1}{\sqrt{2\cosh \Gamma_n}} \begin{pmatrix} e^{\pm \gamma_n/2} \\ \sigma_n e^{\mp \gamma_n/2} \end{pmatrix}, \tag{5.3}$$

$$e^{\gamma_n} = \frac{|E_n| + \xi_n}{\Delta}, \quad \Gamma_n = \mathrm{Re}\ \gamma_n,$$

$$\xi_n = \begin{cases} \sqrt{E_n^2 - \Delta^2}, & |E_n| > \Delta, \\ i\sigma_n \sqrt{\Delta^2 - E_n^2}, & |E_n| < \Delta. \end{cases} \tag{5.4}$$

To find the scattering amplitudes in Eq. (5.2) we consider the boundary condition Eq. (2.8). It is important to mention that this boundary condition was derived without regard for the energy dispersion of the normal electron scattering amplitudes d and r, which means that now this assumption should be valid for the entire interval of relevant energies E_n. Let us first discuss $j = 1$ (hole-like quasi-particle coming from the left):

$$\begin{aligned} &\begin{pmatrix} 1 \\ 0 \end{pmatrix} u_n^- \delta_{n,0} + \begin{pmatrix} a \\ b \end{pmatrix}_{1,n} u_n^+ \\ &\quad = r \begin{pmatrix} c \\ f \end{pmatrix}_{1,n} u_n^- + \frac{d}{2} \begin{pmatrix} 1+\sigma_z & 0 \\ 0 & 1-\sigma_z \end{pmatrix} \begin{pmatrix} f \\ c \end{pmatrix}_{1,n-1} u_{n-1}^- \\ &\quad + \frac{d}{2} \begin{pmatrix} 1-\sigma_z & 0 \\ 0 & 1+\sigma_z \end{pmatrix} \begin{pmatrix} f \\ c \end{pmatrix}_{1,n+1} u_{n+1}^- . \end{aligned} \tag{5.5}$$

It is convenient to separate the equations for normal and Andreev scattering amplitudes in Eq. (5.5) using a procedure similar to Eq. (3.8). The equation for the normal scattering amplitudes then becomes

$$\begin{aligned} &r c_{1,n} + (d/2)(V_{nn+1}^- f_{1,n+1} + V_{nn-1}^+ f_{1,n-1}) = \delta_{n0}, \\ &r f_{1,n} + (d/2)(V_{nn+1}^+ c_{1,n+1} + V_{nn-1}^- c_{1,n-1}) = 0, \end{aligned} \tag{5.6}$$

where the coefficients

$$V_{nm}^{\pm} = \frac{(u_n^{-*}, \sigma_z \pm 1, u_m^-)}{(u_n^{-*}, \sigma_z u_n^-)} \tag{5.7}$$

have the explicit form

$$V_{nm}^+ = -\frac{\exp(-(\gamma_n + \gamma_m)/2)}{\sinh \gamma_n} \left(\frac{\cosh \Gamma_n}{\cosh \Gamma_m} \right)^{1/2}, \tag{5.8a}$$

$$V_{nm}^- = \sigma_n \sigma_m \frac{\exp((\gamma_n + \gamma_m)/2)}{\sinh \gamma_n} \left(\frac{\cosh \Gamma_n}{\cosh \Gamma_m} \right)^{1/2}. \tag{5.8b}$$

The equation for the Andreev scattering amplitudes is

$$\begin{aligned} &a_{1,n} = (d/2)(U_{nn+1}^- f_{1,n+1} + U_{nn-1}^+ f_{1,n-1}), \\ &b_{1,n} = (d/2)(U_{nn+1}^+ c_{1,n+1} + U_{nn-1}^- c_{1,n-1}), \end{aligned} \tag{5.9}$$

where the coefficients are defined as

$$U_{nm}^{\pm} = \frac{(u_n^{+*}, \sigma_z \pm 1, u_m)}{(u_n^{+*}, \sigma_z u_n^+)}, \tag{5.10}$$

and have the explicit forms

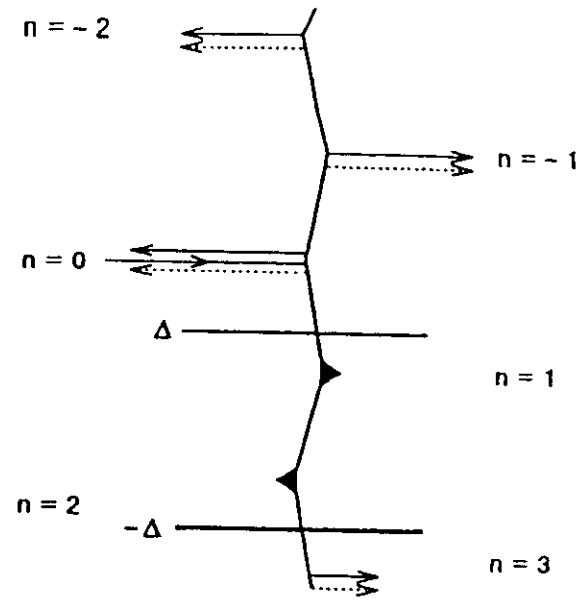

FIG. 4. Scattering diagram of voltage-biased superconducting tunnel junctions. Solid (dotted) arrows indicate scattering in the normal (Andreev) channel. Filled triangles indicate superconducting bound states. Transmission (reflection) occurs into side bands with odd (even) indices.

$$U_{nm}^+ = \frac{\exp((\gamma_n - \gamma_m)/2)}{\sinh \gamma_n} \left(\frac{\cosh \Gamma_n}{\cosh \Gamma_m} \right)^{1/2}, \tag{5.11a}$$

$$U_{nm}^- = -\sigma_n \sigma_m \frac{\exp(-(\gamma_n - \gamma_m)/2)}{\sinh \gamma_n} \left(\frac{\cosh \Gamma_n}{\cosh \Gamma_m} \right)^{1/2}. \tag{5.11b}$$

As can be seen from Eqs. (5.6) and (5.9), the inelastic scattering possesses a specific asymmetry: the forward scattered waves have odd side band indices and backward scattered waves have even side band indices, as illustrated in Fig. 4. Correspondingly, bound states with odd or even side band indices are induced either in the right or in the left electrode. We note that the scattering to any side band consists of normal and Andreev components.

It is instructive to compare the superconducting scattering diagram in Fig. 4 with the scattering diagram of normal junctions. In the normal limit $\Delta = 0$, all the Andreev amplitudes in Eq. (5.9) vanish [$U_n^{\pm} = 0$ in Eq. (5.11)] and Eq. (5.6) split because $V^+ = 0$ in Eq. (5.8), which yields $f_n = c_{n-1} = 0$ for all $n \neq 1$. Thus, the side band diagram in Fig. 4 reduces to the elementary fragment shown in Fig. 5a. This fragment corresponds to the scattering of a *true hole*, meaning a particle with spectrum $E_h = -(p^2/2m - \mu)$, according to the BdG equations (2.2) and (2.5). In the ground state, $T = 0$, these holes fill all positive energy states $E > 0$, while the negative energy states are empty. For the electrons, the corresponding diagram is sketched in Fig. 5b. In this diagram the chemical potentials in both electrodes are equal, while the energies of the incident and transmitted states are shifted by eV. This difference from the conventional diagram of normal electron tunneling in Fig. 5c (where the chemical potentials in the electrodes are shifted relative to each other, while the scattering is elastic) appears after separating out the superconducting phase in Eq. (2.4); the con-

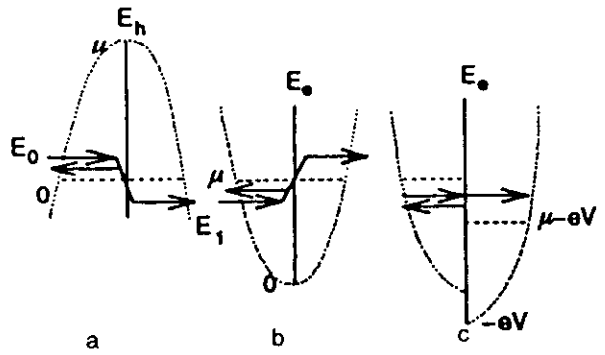

FIG. 5. Scattering diagrams of voltage-biased normal tunnel junctions: scattering of normal holes with spectrum $E_h = \mu - (p^2/2m)$; represents an elementary fragment of the diagram in Fig. 4 for $j = 1$ (a); scattering of the normal electrons with spectrum $E_e = p^2/2m$ (c); conventional diagram of elastic electron scattering in biased tunnel junctions; the local chemical potentials in the electrodes are then shifted by eV (c).

ventional picture with shifted chemical potential can be restored by means of the gauge transformation of the normal electron wave function $\psi \to \exp(-ieVt)\psi$.

When superconductivity is switched on, $\Delta \neq 0$, the incoming quasi-particle consists of both electron and hole components, and therefore the scattering diagram is a combination of the diagrams in Figs. 5,a and 5,b. The electron-hole conversion, which leads to the appearance of electron and hole components in the upper and lower transmitted states, must also be taken into account. Continuation of this process creates the whole superconducting scattering diagram in Fig. 4.

From a mathematical point of view, Eqs. (5.6) and (5.9) for the scattering amplitudes are second-order difference equations which cannot be solved exactly, except in special cases, e.g., a fully transparent constriction ($r=0$), where Eq. (5.6) reduces to a binary relation.[34] In general, it is possible to find asymptotic solutions using a small parameter. In the present case of a tunnel junction, there is a natural small parameter—the transparency of the tunnel barrier: $D \ll 1$. However, a straightforward perturbation expansion with respect to this parameter gives rise to divergences, which are similar to the difficulties encountered in of the multiparticle tunneling theory (MPT).[42,57,58] In order to formulate an improved perturbation procedure, it is convenient to rewrite Eqs. (5.6) and (5.9) in terms of the parameter $\lambda = D/4R$, the true small parameter of the theory, as will be seen later. Accordingly, we introduce new scattering amplitudes

$$c_{1,\pm 2k} = \frac{\lambda^k}{r} c_{\pm 2k}, \quad f_{1,\pm(2k+1)} = \frac{\lambda^k d^*}{2R} f_{\pm(2k+1)},$$

$$a_{1,\pm 2k} = \lambda^k a_{\pm 2k}, \quad b_{1,\pm(2k+1)} = \frac{\lambda^k d}{2r} b_{\pm(2k+1)}, \tag{5.12}$$

which satisfy equations

$$\begin{aligned} &c_n + \lambda V^{-1}_{nn+1} f_{n+1} + V^{+}_{nn-1} f_{n-1} = 0, \\ &f_n - \lambda V^{+}_{nn+1} c_{n+1} - V^{-}_{nn-1} c_{n-1} = 0, \\ &a_n = \lambda U^{-}_{nn+1} f_{n+1} + U^{+}_{nn-1} f_{n-1}, \end{aligned} \tag{5.13a}$$

$$b_n = \lambda U^{+}_{nn+1} c_{n+1} + U^{-}_{nn-1} c_{n-1} \tag{5.13b}$$

for $n>0$. For $n<0$ it is necessary to make the change $V^{\pm}_{nm} \to V^{\mp}_{-n-m}$, $U^{\pm}_{nm} \to U^{\mp}_{-n-m}$, $(n, m>0)$ in the above equations. The equation for $n = 0$ can then be written as

$$c_0 + \lambda(V^{-}_{01} f_1 + V^{+}_{0-1} f_{-1}) = 1. \tag{5.13c}$$

Let us now turn to the second scattering case in Eq. (5.2), $j=2$ (hole-like quasi-particle incoming from the right). According to the symmetry relations of Eq. (3.6), the scattering amplitudes $j=2$ differ from the scattering amplitudes $j=1$ by $\varphi \to -\varphi$, which in our time-dependent case means that $n \pm 1 \to n \mp 1$. Taking into account this symmetry and also the property of the scattering amplitudes in Eq. (3.6), we introduce new scattering amplitudes

$$f_{2,\pm 2k} = \frac{\lambda^k}{r} \bar{c}_{\pm 2k},$$

$$c_{2,\pm(2k+1)} = \frac{\lambda^k d^*}{2R} \bar{f}_{\pm(2k+1)}, \quad b_{2,\pm 2k} = \lambda^k \bar{a}_{\pm 2k}, \tag{5.14}$$

which satisfy the following equations (for $n > 0$):

$$\begin{aligned} &\bar{c}_n + \lambda V^{+}_{nn+1} \bar{f}_{n+1} + V^{-}_{nn-1} \bar{f}_{n-1} = 0, \\ &\bar{f}_n - \lambda V^{-}_{nn+1} \bar{c}_{n+1} - V^{+}_{nn-1} \bar{c}_{n-1} = 0, \\ &\bar{a}_n = \lambda U^{+}_{nn+1} \bar{f}_{n+1} + U^{-}_{nn-1} \bar{f}_{n-1}, \end{aligned} \tag{5.15a}$$

$$\bar{b}_n = \lambda U^{-}_{nn+1} \bar{c}_{n+1} + U^{+}_{nn-1} \bar{c}_{n-1}, \tag{5.15b}$$

$$\bar{c}_0 + \lambda(V^{+}_{01} \bar{f}_1 + V^{-}_{0-1} \bar{f}_{-1}) = 1. \tag{5.15c}$$

Equations (5.15) differ from Eqs. (5.13) by

$$V^{\pm} \to V^{\mp}, U^{\pm} \to U^{\mp}. \tag{5.16}$$

In the case of electron-like quasi-particles incoming from the left, $j=3$, the symmetry of Eq. (3.7) involves transformation $\gamma \to -\gamma$, which means transformation of the coefficients $V^{\pm} \to -\sigma_n \sigma_m V^{\mp}$, $U^{\pm} \to -\sigma_n \sigma_m U^{\mp}$ in Eqs. (5.6) and (5.9). This transformation allows us to relate the scattering amplitudes of this case to the solutions of Eqs. (5.5):

$$a_{3,\pm 2k} = \frac{\lambda^k}{r^*} \sigma_{\pm 2k} \bar{c}_{\pm 2k},$$

$$b_{3,\pm(2k+1)} = -\frac{\lambda^k d}{2R} \sigma_{\pm(2k+1)} \bar{f}_{\pm(2k+1)},$$

$$c_{3,\pm 2k} = \lambda^k \sigma_{\pm 2k} \bar{a}_{\pm 2k}, \tag{5.17}$$

$$f_{3,\pm(2k+1)} = -\frac{\lambda^k d^*}{2r^*} \sigma_{\pm(2k+1)} \bar{b}_{\pm(2k+1)}.$$

In a similar way the scattering amplitudes of electron-like quasi-particles incoming from the right, $j=4$, are related to the solutions of Eqs. (5.13):

$$b_{4,\pm 2k} = \frac{\lambda^k}{r^*} \sigma_{\pm 2k} c_{\pm 2k},$$

$$a_{4,\pm(2k+1)} = -\frac{\lambda^k d}{2R} \sigma_{\pm(2k+1)} f_{\pm(2k+1)},$$

$$f_{4,\pm 2k}=\lambda_k\sigma_{\pm 2k}a_{\pm 2k},$$

$$c_{4,\pm(2k+1)}=-\frac{\lambda^k d^*}{2r^*}\sigma_{\pm(2k+1)}b_{\pm(2k+1)}. \tag{5.18}$$

According to the symmetry of the coefficients in Eqs. (5.13) and (5.15),

$$V^{\pm}_{nm}(-E)=V^{\pm *}_{-n-m}(E),\quad U^{\pm}_{nm}(-E)=U^{\pm *}_{-n-m}(E), \tag{5.19}$$

all scattering amplitudes with positive and negative incoming energies are related by the relation

$$a_n(-E)=\bar{a}_{-n}{}^*(E), \tag{5.20}$$

and similarly for the other amplitudes.

Let us now formally solve Eq. (5.13) for $n>0$ in the form[55]

$$f_{2k+1}=(-1)^k\prod_{i=0}^{2k+1}S_i c_0, \tag{5.21}$$

where the quantities S_l are defined as

$$S_{2k}=-\frac{c_{2k}}{f_{2k-1}},\quad S_{2k+1}=\frac{f_{2k+1}}{c_{2k}}, \tag{5.22}$$

and satisfy the recurrence relations

$$S_{2k}=\frac{V^{+}_{2k,2k-1}}{1+\lambda V^{-}_{2k,2k+1}S_{2k+1}},$$

$$S_{2k+1}=\frac{V^{-}_{2k+1,2k}}{1+\lambda V^{+}_{2k+1,2k+2}S_{2k+2}}. \tag{5.23}$$

The quantity c_0 in Eq. (5.27) is given by

$$c_0=\frac{1}{1+\lambda(V^{-}_{01}S_1+V^{+}_{0-1}S_{-1})}. \tag{5.24}$$

It is convenient to express the functions S_n in Eq. (5.23) in terms of the relation $S_n=V^{\pm}_{n,n+1}/Z_n$, where the denominators $Z_n(n\neq 0)$ satisfy the recurrence relation

$$Z_n=1+\lambda\frac{a^{\pm}_n a^{\pm}_{n+1}}{Z_{n+1}},\quad a^{\pm}_n=\frac{e^{\pm\gamma_n}}{\sinh\gamma_n}, \tag{5.25}$$

($\pm$ corresponds to even/odd n), and to define Z_0 as the denominator of c_0, Eq. (5.24):

$$Z_0=1+\lambda\frac{a^{+}_0 a^{+}_1}{Z_1}+\lambda\frac{a^{-}_0 a^{-}_{-1}}{Z_{-1}}. \tag{5.26}$$

Using the above notation, we can express the coefficients of the normal forward scattering, $|f_n|^2$, in the form

$$|f_n|^2=\frac{e^{\gamma_0}}{\cosh\gamma_0|Z_0|^2}e^{\Gamma_n}\cosh\Gamma_n\prod_{l=1}^{n}\frac{1}{|Z_l\sinh\gamma_l|^2}. \tag{5.27}$$

The equation for the coefficients of the normal backward scattering, $|c_n|^2$, differs from Eq. (5.27) by $\exp(\Gamma_n)\cdot\exp(-\Gamma_n)$. The relation between the amplitudes of the Andreev and normal forward scattering in Eq. (5.13) taking into account Eqs. (5.22), (5.23), and (5.25), has the form

$$b_n=-e^{-\gamma_n}\left(1-\lambda\frac{2e^{-\gamma_{n+1}}}{\sinh\gamma_{n+1}Z_{n+1}}\right)f_n. \tag{5.28}$$

In a similar way, one can express the solution of Eq. (5.15) for $n>0$ in the form

$$|\bar{f}_n|^2=\frac{e^{-\gamma_0}}{\cosh\gamma_0|\bar{Z}_0|^2}e^{-\Gamma_n}\cosh\Gamma_n\prod_{l=1}^{n}\frac{1}{|\bar{Z}_l\sinh\gamma_l|^2},$$

$$\bar{b}_n=-e^{\gamma_n}\left(1+\lambda\frac{2e^{\gamma_{n+1}}}{\sinh\gamma_{n+1}\bar{Z}_{n+1}}\right)\bar{f}_n, \tag{5.29}$$

where

$$\bar{Z}_n=1+\lambda\frac{a^{\mp}_n a^{\mp}_{n+1}}{\bar{Z}_{n+1}},$$

$$\bar{Z}_0=1+\lambda\frac{a^{-}_0 a^{-}_1}{\bar{Z}_1}+\lambda\frac{a^{+}_0 a^{+}_{-1}}{\bar{Z}_{-1}}. \tag{5.30}$$

We note that Eqs. (5.29) and (5.30) differ from Eqs. (5.27) and (5.28) by $\gamma_n\to-\gamma_n$ everywhere.

Equations for the scattering amplitudes with negative side band indices, $n<0$, can be derived in a similar way, and the result differs from the above equations for positive side band indices [Eqs. (5.25)–(5.30)] by the substitution

$$\gamma_n\to-\gamma_{-|n|},\quad n\neq 0, \tag{5.31}$$

which is introduced everywhere except in Z_0 and $\bar{Z}_0$.

6. QUASIPARTICLE CURRENT

In the nonstationary problem under consideration, the density matrix determining the current [Eq. (4.1)] is time dependent, and its dynamic evolution can be described by an equation similar to Eq. (4.3),

$$\langle\hat{\Psi}(\mathbf{r},t)\hat{\Psi}^{+}(\mathbf{r},t)\rangle=\sum_{\lambda}\Psi_\lambda(\mathbf{r},t)f_\lambda\Psi^{+}_\lambda(\mathbf{r},t), \tag{6.1}$$

Ψ_λ are now solutions of the time-dependent problem, Eq. (2.5), whose initial conditions correspond to the eigenstates of the initial Hamiltonian with the eigenvalues λ, and occupation numbers f_λ of these initial states. We consider the inelastic scattering states, [Eqs. (2.6) and (5.2)] as the propagators $\Psi_\lambda(t)$ in Eq. (6.1) with λ corresponding to the complete set of the incoming states $\lambda=(E,j)$; according to the assumption about local equilibrium within the electrodes, the incoming states possess the Fermi distribution of occupation numbers, $f_{Ej}=n_F(-E)$. Thus the current [Eq. (4.1)] takes the form

$$I(t)=-e\int_{|E|>\Delta}\frac{d|E|}{2\pi\xi}n_F(-E)\sum_{N=-\infty}^{\infty}e^{iNeVt}$$
$$\times\sum_{n=-\infty}^{\infty}\sum_{j\beta}\beta(\psi^{\beta}_j(E,n),\psi^{\beta}_j(E,N+n)). \tag{6.2}$$

The current in Eq. (6.2) consists of a time-independent part, $N=0$, which is formed by incoherent contributions from all the side bands (the quasiparticle current) and from a time-dependent part, $N\neq 0$, which results from interference among

the different side bands (Josephson alternating current). The difference between the side band indices N is an even number since the side band index is either even or odd, depending on the electrode; therefore, the time-dependent current oscillates with the Josephson frequency $\omega = 2eV$.

In this paper we concentrate on an analysis of the time-dependent quasiparticle current. By analogy with Eq. (4.7), we calculate the current using the transmitted states,

$$I = \frac{1}{2}\frac{e}{\pi}\int_{|E|>\Delta} dE\,\frac{|E|}{\xi}\,n_F(-E)\sum_{n=-\infty}^{\infty} \times\left[\sum_{j=1,3}(|f_{jn}|^2-|b_{jn}|^2)+\sum_{j=2,4}(|a_{jn}|^2-|c_{jn}|^2)\right]. \tag{6.3}$$

Using the scattering amplitudes introduced in the previous section through Eqs. (5.12), (5.14), (5.17), and (5.18), we express the current in Eq. (6.3) in the form

$$I = \frac{e}{\pi}\int_{|E|>\Delta} dE\,\frac{|E|}{\xi}\,n_F(-E)\sum_{\text{odd}}(K_n-\bar{K}_n), \tag{6.4}$$

where

$$K_n = \lambda^{|n|}(R^{-1}|f_n|^2-|b_n|^2),$$
$$\bar{K}_n = \lambda^{|n|}(R^{-1}|\bar{f}_n|^2-|\bar{b}_n|^2) = K_n(-\gamma). \tag{6.5}$$

The factor of 2 appears in Eq. (6.4) because of equality of the currents I_1 and I_4 and the currents I_2 and I_3 in Eq. (4.8), which hold also in the nonstationary case. However, there is no balance between the currents of these two pairs any more. The symmetry of Eq. (5.20) allows us to reduce the interval of integration in Eq. (6.4) to the semiaxis $E > 0$,

$$I = \frac{e}{\pi}\int_{\Delta}^{\infty} dE\,\frac{E}{\xi}\tanh\frac{E}{2T}\sum_{\text{odd}}(K_n-\bar{K}_n). \tag{6.6}$$

The side band currents K_n in Eq. (6.5) are proportional to the powers of the small parameter λ, $K_n \sim \lambda^{|n|}$. Therefore, Eqs. (6.6) and (6.5) present a perturbative expansion of the current, which is convenient for analysis in the limit of low barrier transparency. In the following sections we carry out such an analysis of the structure of the current in Eq. (6.6).

7. EXCESS CURRENT AT LARGE BIAS

To make some useful observations for analysis of the subgap current, it is instructive first to discuss the simpler case of large bias $eV \gg \Delta$, which has been studied extensively in literature.[11,12,17,23] We derive at the same time the explicit analytical expression for the current in this limit, which is valid in the whole range of the junction transparency, $0 < D < 1$. The asymptotic expansion of the current with respect to the small parameter Δ/eV has the form[17]

$$I = \frac{e^2 DV}{\pi} + I_{\text{exc}}(D) + O\left(\frac{\Delta}{eV}\right), \tag{7.1}$$

where the first term is the tunnel current of the normal junction and the second term is a voltage-independent excess current which represents the leading superconducting correction.

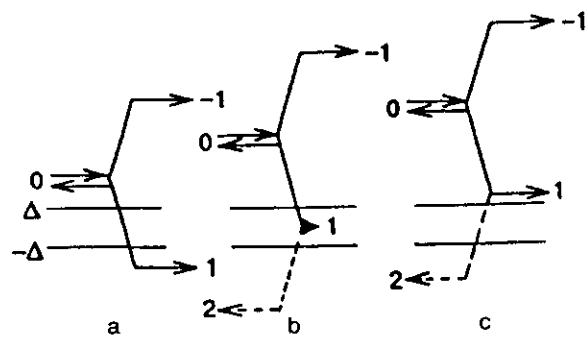

FIG. 6. Three kinds of processes that contribute to the tunnel current at large bias $eV \gg \Delta$: creation of a real excitation across the gap by forward scattering (a); excitation of the Andreev bound state due to creation of a real excitation via backward scattering (dashed arrow) (b); imbalance of ground state modes due to creation of a real excitation via backward scattering (c). Excess current is caused by processes b) and c).

A main simplification in this case is that the side band currents K_n and $\bar{K}_n$, $|n| > 1$ diminish when the bias voltage increases. This follows from an estimate of the transmission amplitudes in Eqs. (5.27)–(5.29), which contain products of factors $|\sinh\gamma_k|^{-2}$ which are small at large voltages, $|\sinh\gamma_k|^{-2} \sim (\Delta/eV)^2$, because of the large interval of involved energies, $E \sim eV$. Furthermore, inspection of the amplitudes f_{-1} and $\bar{f}_1$ shows that they are also small due to the factors $\exp(-\gamma_0-\gamma_1)$; therefore, the nonvanishing part of the current [Eq. (6.6)] in the limit $eV \gg \Delta$ becomes

$$I = \frac{e}{\pi}\int_{\Delta}^{\infty} dE\,\frac{E}{\xi}\tanh\frac{E}{2T}(K_1-\bar{K}_{-1}). \tag{7.2}$$

The essential fragments of the scattering diagram in the large bias limit are shown in Fig. 6.

The structure of the current in Eq. (7.2) is essentially determined by the presence of a gap in the spectrum of the side band $n = 1$; this causes different analytical forms of the current K_1 in the regions $|E| < \Delta$ and $|E| > \Delta$. We note that the spectrum of the side band $n = -1$ possesses no gap: $E_{-1} > \Delta$ for $E > \Delta$. Accordingly, we divide the integral in Eq. (7.2) into three parts:

$$I = I_< + I_\Delta + I_> .$$

The first part corresponds to the current of the states in the side band $n = 1$, which lie below the gap, $E_1 < -\Delta$. The second part corresponds to the current of the states of the same side band which lie in the gap, $-\Delta < E_1 < \Delta$. The third part combines contributions from the remaining states of the side band $n = 1$, $\Delta < E_1$, and from all the states of the side band $n = -1$. Making use of the approximations

$$|Z_0|^2 = |\bar{Z}_0|^2 \approx |1+2\lambda(E+\xi)/\xi|^2,$$
$$|Z_{-1}|^2 = |\bar{Z}_1|^2 = |Z_2|^2 = |\bar{Z}_{-2}|^2 \approx 1, \tag{7.3}$$
$$|Z_1|^2 = |\bar{Z}_{-1}|^2 = |Z_{-2}|^2 = |\bar{Z}_2|^2 \approx 1/R^2,$$

it is possible to express the integral $I_<$ in the form (we restrict the analysis to the limit $T = 0$):

$$I_< = \frac{e}{\pi}\int_{\Delta}^{eV-\Delta} dE\,\frac{E}{\xi}K_1 = \frac{8e\lambda}{\pi R}\int_{\Delta}^{eV/2} dE\,\frac{E}{\xi Z_0^2} - \frac{2e\lambda}{\pi R}\int_{\Delta}^{\infty} dE\,\frac{(E-\xi)}{\xi Z_0^2}\left(1-4\lambda R\,\frac{E}{\xi}\right), \qquad (7.4)$$

where the limit of integration in the last term is extended to infinity since the main contribution to this integral comes from the energies $E \sim \Delta \ll eV$. Separating out the normal junction current, we can express Eq. (7.4) in the form

$$I_< = \frac{e^2DV}{\pi} - \frac{8e\lambda^2}{\pi}\int_{\Delta}^{\infty}\frac{dE}{Z_0^2\xi}\left[4\lambda R\,\frac{E\Delta^2}{\xi^2} + (2R+1)\,\frac{E(E-\xi)}{\xi} + \frac{E-\xi}{4\lambda R}\right]. \qquad (7.5)$$

We note that this current is always smaller than the normal current. It is convenient to express the integral I_Δ as

$$I_\Delta = \frac{e}{\pi}\int_{eV-\Delta}^{eV+\Delta} dE\,\frac{E}{\xi}K_1 = \frac{16e\lambda^2}{\pi}\int_0^{\Delta} dE\,\frac{\Delta^2}{|\xi Z_0|^2}, \qquad (7.6)$$

which is found from the relations between the functions Z_n [which result from their definition in Eq. (5.25)]

$$Z_n(E+eV) = \bar{Z}_{n-1}(E),$$

$$Z_0(E+eV)Z_1(E+eV) = \bar{Z}_0(E)\bar{Z}_{-1}(E). \qquad (7.7)$$

Inspection of the equation for $I_>$,

$$I_> = \frac{e}{\pi}\int_{eV+\Delta}^{\infty} dE\,\frac{E}{\xi}K_1 - \frac{e}{\pi}\int_{\Delta}^{\infty} dE\,\frac{E}{\xi}\bar{K}_{-1}, \qquad (7.8)$$

shows that the two integrals diverge at the upper limit $E \to \infty$, which means that the states lying far from the Fermi level formally contribute to the current, while the quasiclassical approximation of Eq. (2.6) assumes that all relevant states lie close to the Fermi level. To eliminate this formal divergence, the variable is commonly shifted by eV in the first integral in Eq. (7.8). Using again the relations (7.7) we express this integral in the form

$$\frac{4e\lambda}{\pi R}\int_{\Delta}^{\infty} dE\,\frac{E}{\xi Z_0 Z_{-1}} + \frac{8e\lambda^2}{\pi}\int_{\Delta}^{\infty} dE\,\frac{E(E-\xi)}{\xi^2 Z_0^2},$$

where the first term has the same analytical form but the opposite sign compared to the divergent term in the second integral in Eq. (7.8),

$$\frac{4e\lambda}{\pi R}\int_{\Delta}^{\infty} dE\,\frac{E}{\xi Z_0 Z_{-1}} + \frac{2e\lambda}{\pi R}\int_{\Delta}^{\infty} dE\,\frac{(E-\xi)}{\xi Z_0^2}.$$

After elimination of the divergent terms, the integral in Eq. (7.8) takes the form

$$I_> = \frac{2e\lambda}{\pi R}\int_{\Delta}^{\infty} dE\,\frac{(E-\xi)}{\xi Z_0^2}\left(1+4\lambda R\,\frac{E}{\xi}\right). \qquad (7.9)$$

The positive currents in Eq. (7.9) and Eq. (7.6) overcompensate the missing part of the current in Eq. (7.5). Collecting Eqs. (7.5), (7.6), and (7.9), we find after some algebra the following explicit equation for the excess current in Eq. (7.1)

$$I_{exc} = \frac{16e\Delta\lambda^2 R}{\pi}\left[1 - \frac{D^2}{2(1+R)\sqrt{R}}\ln\frac{1+\sqrt{R}}{1-\sqrt{R}}\right], \qquad (7.10)$$

which is valid in the whole interval of junction transparency $0 < D \leq 1$. Asymptotics of this expression coincide with the results presented in literature,[11,23] both in the limit of fully transparent ($D = 1$) constrictions, $I_{exc} = 8e\Delta/3\pi$, and in the limit of low-transparency ($D \ll 1$) tunnel junctions, $I_{exc} = e\Delta D^2/\pi$.

The above calculation reveals an important difference between the structure of the current in normal and superconducting junctions. In normal junctions, the current, e.g., in the right electrode (see Fig. 5c) results from scattering states that lie above the local chemical potential, $E > \mu - eV$, while contribution from the energy interval $E < \mu - eV$ is equal to zero due to mutual cancellation of currents of the scattering states incident from the left and from the right (in Fig. 5a the current-carrying energy region corresponds to negative energies, $E_h < 0$). Thus, the total current coincides with the current of real excitations emitted from the contact, which is consistent with the nonequilibrium origin of the current in the voltage-biased junctions. In superconducting junctions, only "across-the-gap" current $I_<$ is clearly related to the real excitations emitted at the right side of the junction where the current is calculated (Fig. 6a): the dissipative character of the currents, I_Δ and $I_>$, is not obvious. However, the creation of real excitations at the left side of the junction via backscattering into the side band $n = 2$ should be taken into account (Figs. 6b and 6c). Although the current of this side band exists only at the left side of the scattering diagram, it should have an effect at the right side due to continuity of the current at the interface [Eq. (4.5)] and therefore it should be distributed among the states of the side band $n = 1$. As our calculations show, this "kick" current partially flows through the Andreev bound states, which involve the current I_Δ (Fig. 6b) and which convert this current into a supercurrent outside the junction. It is also partially distributed among the scattering states with positive energies (current $I_<$, Fig. 6c) in the form of imbalanced ground state currents.

8. SUBGAP CURRENT

In this section we discuss the tunnel current in the subgap region, $eV < 2\Delta$. A basic property of the subgap current is the presence of temperature-independent structures on the I–V characteristics – the subharmonic gap structure (SGS). The SGS in tunnel junctions was discovered in experiments by Taylor and Burstein[56] and the first theoretical explanation was given by Schrieffer and Wilkins[42] in terms of multiparticle tunneling (MPT). Recently, the SGS has been observed in many experiments on transmissive tunnel junctions.[1–5] Although SGS in planar junctions can be attributed to normal shorts, the observation of SGS in superconducting controllable break junctions[8] provided convincing confirmation of the existence of SGS in the true tunnel regime.

The existence of SGS in tunnel current can be established within the MPT theory by means of rather simple perturbative arguments.[42,57,58] Assuming a small perturbative coupling between electrodes, we can calculate, on the

basis of the tunnel Hamiltonian model, the probability of tunneling in nth order of perturbation theory. Such a probability is proportional to a product of filling factors of the initial and the final states: $n_F(E)[1 - n_F(E - neV)]$. At zero temperature this factor is equal to zero outside the interval $\Delta < E < neV - \Delta$, which selects the quasiparticle transitions across the gap, i.e., the processes of creation of real excitations relevant for the tunnel current. Such a restriction places the threshold of the nth order current at $eV = 2\Delta/n$, and a sequence of current onsets of $\sim D^n$ at the voltages $eV = 2\Delta/n$ forms the SGS of the tunnel current.[58,59]

In our approach, the filling factors of final states do not enter the equation for the current Eq. (6.6), and the existence of SGS is therefore not obvious, although the side band currents [Eq. (6.5)] gradually decrease with increasing side band index. However, attribution of the nonequilibrium tunnel current in biased junctions to the current of real excitations is a general physical argument which should be automatically met in any correct theory. In fact, the true tunnel current, as we can see from the discussion of the previous section, is hidden in Eq. (6.6): it results from partial cancellation of large contribution of different scattering modes. The cancellation is nontrivial because of mixture of currents of different side bands, the odd side bands containing information about the currents of the even side bands and vice versa. This means that a finite perturbation expansion of Eq. (6.6) is not satisfactory and will not adequately correspond to the perturbative structure of the true tunnel current. To reveal such a structure one must rearrange the series in Eq. (6.6).

To this end, we consider a general term K_n, $n > 0$ in Eq. (6.6). It follows immediately from the explicit form of the normal and Andreev transmission coefficients [Eqs. (5.27) and (5.28)] that the leading term with respect to λ in K_n is proportional to a factor $[(1 - \exp(2\Gamma_n)]$, which is equal to zero if $|E_n| < \Delta$. Having made this observation, we express the quantity K_n in the form

$$K_n = \frac{2}{R}\lambda^n \theta(E_n^2 - \Delta^2) e^{-\gamma_n} \sinh \gamma_n |f_n|^2 + 4\lambda^{n+1} e^{-2\Gamma_n} \left| \frac{f_n}{Z_{n+1}} \right|^2 F_{n+1}, \tag{8.1a}$$

$$F_{n+1} = |Z_{n+1}|^2 + \mathrm{Re}\left(\frac{e^{-\gamma_{n+1}} Z_{n+1}^*}{\sinh \gamma_{n+1}} \right) - \lambda \left| \frac{e^{-\gamma_{n+1}}}{\sinh \gamma_{n+1}} \right|^2. \tag{8.1b}$$

In Eq. (8.1a) the first term represents the main contribution of the nth side band to the current: it is proportional to the probability of normal scattering to the nth side band and it does not contain the contribution of the side band states lying inside the gap $|E_n| < \Delta$. Using the recurrence relation (5.25) and recalling that $\lambda = D/4R$, after some algebra the function F_n in Eq. (8.1b) becomes

$$F_n = \frac{1}{R}\theta(E_n^2 - \Delta^2) \frac{1}{\tanh \gamma_n} + \lambda \left| \frac{e^{\gamma_n}}{\sinh \gamma_n Z_{n+1}} \right|^2 G_{n+1}, \tag{8.2a}$$

$$G_{n+1} = |Z_{n+1}|^2 - \mathrm{Re}\left(\frac{e^{\gamma_{n+1}} Z_{n+1}^*}{\sinh \gamma_{n+1}} \right) - \lambda \left| \frac{e^{\gamma_{n+1}}}{\sinh \gamma_{n+1}} \right|^2. \tag{8.2b}$$

Substituting Eq. (8.2) into Eq. (8.1a), we find that the second term in the equation for K_n, which is proportional to λ^{n+1}, has analytical structure similar to the first term in the same equation, proportional to λ^n, namely, it consists of the probability of normal scattering to the $(n + 1)$th side band [cf. Eq. (5.22)] and it does not include the contribution of the side band states that lie inside the gap, $|E_{n+1}| < \Delta$. This allows us to associate this term with the effective contribution of the nearest *even* side band.

A similar transformation of the function G_{n+1} in Eq. (8.2) yields the recurrence relation

$$G_{n+1} = -\frac{1}{R}\theta(E_{n+1}^2 - \Delta^2) \frac{1}{\tanh \gamma_{n+1}} - \lambda \left| \frac{\exp(-\gamma_{n+1})}{\sinh \gamma_{n+1} Z_{n+2}} \right|^2 F_{n+2}. \tag{8.3}$$

Combining of Eqs. (8.1a)–(8.3) shows that the next term of the current K_n, which is proportional to λ^{n+2}, has the same analytical structure as the leading term in the current K_{n+2} of the next odd side band, and therefore it can be regarded as a renormalization of that current.

Continuing this procedure by systematic use of the recurrence relations (8.2) and (8.3), we obtain the following expansion for the current K_n in Eq. (6.5):

$$\begin{aligned} K_n = {} & \frac{2\lambda^n}{R}\theta(E_n^2 - \Delta^2) Q_n + \frac{4\lambda^{n+1}}{R}\theta(E_{n+1}^2 - \Delta^2) \\ & \times e^{-\Gamma_n} \cosh \Gamma_n Q_{n+1} + \frac{4\lambda^{n+2}}{R}\theta(E_{n+2}^2 - \Delta^2) \\ & \times \exp(-\Gamma_n + 2\Gamma_{n+1}) \cosh \Gamma_n Q_{n+2} + \frac{4\lambda^{n+3}}{R} \\ & \times \theta(E_{n+3}^2 - \Delta^2) \exp(-\Gamma_n + 2\Gamma_{n+1} - 2\Gamma_{n+2}) \cosh \\ & \times \Gamma_n Q_{n+3} + \ldots, \end{aligned} \tag{8.4}$$

where we have introduced the quantity Q_n defined for all n as

$$Q_n = \frac{e^{\gamma_0}}{\cosh \gamma_0 |Z_0|^2} \sinh \gamma_n \cosh \Gamma_n \prod_{l=1}^{n} \frac{1}{|Z_l \sinh \gamma_l|^2}. \tag{8.5}$$

Similar expansions can be derived for the currents K_n and for the currents of the side bands with negative $n < 0$. Expanding each term of the series in Eq. (6.6) with use of Eq. (8.4) and collecting the terms with the same factor λ^n, we can finally express the series in the form

$$\sum_{\text{odd}} (K_n - \bar{K}_n) = \sum_{n \neq 0} (\bar{K}_n - \mathring{K}_n). \tag{8.6}$$

The last summation is done over all odd *and even* integer n, and the renormalized coefficients have the form

$$\tilde{K}_n=\lambda''\theta(E_n^2-\Delta^2)(4Q_n/R)[(1/2)+\cosh\Gamma_{n-2}\times\exp(-\Gamma_{n-2}+2\Gamma_{n-1})+\cosh\Gamma_{n-4}\times\exp(-\Gamma_{n-4}+2\Gamma_{n-3}-2\Gamma_{n-2}+2\Gamma_{n-1})+\ldots+\cosh\Gamma_1\exp(-\Gamma_1+2\Gamma_2-2\Gamma_3+\ldots+2\Gamma_{n-1})] \quad (8.7a)$$

for odd $n>0$ and the form

$$\tilde{K}_n=\lambda''\theta(E_n^2-\Delta^2)(4Q_n/R)[\cosh\Gamma_{n-1}e^{-\Gamma_{n-1}}+\cosh\Gamma_{n-3}\exp(-\Gamma_{n-3}+2\Gamma_{n-2}-2\Gamma_{n-1})+\ldots+\cosh\Gamma_1\exp(-\Gamma_1+2\Gamma_2-2\Gamma_3+\ldots-2\Gamma_{n-1})] \quad (8.7b)$$

for even $n>0$.

The representation of Eqs. (8.6) and (8.7) is exact. A general term of the series can be regarded as an effective renormalized current of the nth side band. In fact, this effective current consists of the contributions of all side bands with odd indices smaller than n. An important feature of this representation is the presence of the θ-function in the general term, which allows us to separate out in Eq. (6.6) that part of the current which is obviously responsible for the SGS,

$$I_{SGS}=\sum_{n=1}^{\infty}\frac{e}{\pi}\int_{\Delta}^{neV-\Delta}dE\,\frac{E}{\xi}\tanh\frac{E}{2T}(\tilde{K}_n-\tilde{K}_n). \quad (8.8)$$

One might expect (cf. Ref. 55) that Eq. (8.8) represents the subgap tunnel current at zero temperature and that the remaining part of the current in Eq. (6.6),

$$I_r=I-I_{SGS}=\sum_{n=1}^{\infty}\frac{e}{\pi}\left[\int_{neV+\Delta}^{\infty}dE\,\frac{E}{\xi}\tanh\frac{E}{2T}(\tilde{K}_n-\tilde{K}_n)+\int_{\Delta}^{\infty}dE\,\frac{E}{\xi}\tanh\frac{E}{2T}(\tilde{K}_n-\tilde{K}_n)\right], \quad (8.9)$$

corresponds to the current of thermal excitations. However, this separation is not exact. An analysis shows that the current in Eq. (8.9) does not vanish completely at $T=0$, but contributes a small residual part. An important property of this residual current is that it does not contain any structureless component but demonstrates behavior similar to the current I_{SGS} in Eq. (8.8), thus resulting in a small correction to Eq. (8.8).

9. SUBHARMONIC GAP STRUCTURE

The explicit analytical expressions (8.8) and (8.9) provide a basis for numerical calculation of the subgap current for small λ (low transparency) with any desirable accuracy. However, they are also convenient for qualitative discussion of the SGS. In this section we will analyze the SGS at zero temperature on the basis of Eq. (8.8).

The current-voltage characteristic $I_{SGS}(V)$ in Eq. (8.8) has a complex form consisting of a sum of renormalized side band currents $I_n(V,\lambda)$:

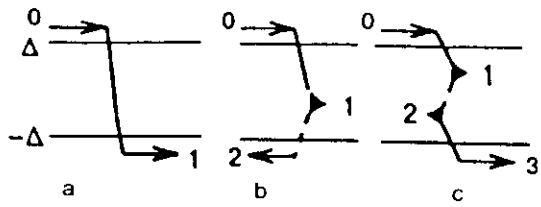

FIG. 7. Scattering processes that contribute to the subgap current: single-particle scattering into the side band $n=1$ gives the main contribution at $eV>2\Delta$ (a); excitation of the Andreev bound state ($n=1$) due to backward scattering into the side band $n=2$ gives the main contribution at $eV>\Delta$ (b); single-particle scattering into the side band $n=3$ and simultaneous excitation of the Andreev bound state in the side band $n=1$ gives the main contribution at $eV>2\Delta/3$ (c).

$$I_{SGS}(V,\lambda)=\sum_{n=1}^{\infty}I_n(V,\lambda),$$

$$I_n(V,\lambda)=\frac{e}{\pi}\int_{\Delta}^{neV-\Delta}dE\,\frac{E}{\xi}(\tilde{K}_n-\tilde{K}_n). \quad (9.1)$$

The partial current-voltage characteristics $I_n(V,\lambda)$ are similar to each other, and it is convenient to analyze them independently.

According to Eq. (9.1) the partial current I_n starts with an onset at the threshold voltage $V_n=2\Delta/en$. In the limit $\lambda\to0$ the onset is infinitely sharp and its magnitude is

$$I_n(V_n,\lambda\to0)=e\Delta D^n\frac{2n}{4^{2n-1}}\frac{n^{2n}}{(n!)^2}. \quad (9.2)$$

The jumps of the current at the thresholds result from the singular denominators in Eqs. (5.27) and (5.29), which are related to the singular density of states at the side band energy gap edges, $\sinh\gamma_k=0$. Accumulation of these singularities in the high-order scattering amplitudes leads to a huge increase of the partial currents well above the corresponding thresholds—this causes the failure of multiparticle tunneling theory.[57-59] In our theory, the singularities are regularized by the factors

$$P_n=\prod_{k=0}^{n}|Z_k|^2 \quad (9.3)$$

in the denominators of the scattering amplitudes, Eq. (5.27). These factors are expressed in terms of the continued fractions Z_n [Eq. (5.25)], which therefore should be calculated with sufficient accuracy to preserve the singular parts of Z_n which provide regularization of the integrals.

The first-order current I_1 in Eq. (9.1) corresponds to direct one-particle scattering to the side band $n=1$ (Fig. 7a). The explicit form of the current I_1 is

$$I_1=\frac{2e\lambda}{\pi R}\int_{\Delta}^{eV-\Delta}dE\,\frac{|E_1|}{\xi\xi_1}\left(\frac{E+\xi}{P_1}+\frac{E-\xi}{\bar{P}_1}\right). \quad (9.4)$$

In the limit $\lambda\to0$ this current coincides with the quasiparticle current of the tunnel Hamiltonian model.[54,60] At finite λ the threshold onset of the current at $V=V_1$ is washed out. To evaluate the width of the onset we truncate the continued fraction in P_1 assuming $Z_{k+1}=Z_k=1$, which yields

$$P_1 \approx |(1+\lambda a_0^- a_{-1}^-)(1+\lambda a_1^- a_2^-)+\lambda a_0^+ a_1^+|^2. \qquad (9.5)$$

The function $\bar{P}_1$ has a similar form. The regularization effect of the threshold singularity is provided by the most singular term $\lambda a_0^+ a_1^+$ in Eq. (9.5). Keeping this term, we obtain in the vicinity of the threshold, $e(V - V_1) \ll \Delta$, the result

$$I_1(V) = \frac{2e\Delta\lambda}{\pi R} f\left(\frac{eV - eV_1}{\Delta\lambda}\right),$$

$$f(z) = \int_0^\pi d\theta \frac{\sin^2\theta}{(\sin\theta + 1/z)^2}. \qquad (9.6)$$

According to this formula the onset width is $e(V - V_1) \sim \lambda\Delta$.

The second-order current I_2 corresponds to the creation of a real excitation during quasiparticle backscattering into the side band $n=2$ (Fig. 7b) and appears as the current of transmitted states of the side band $n=1$ (cf. the excess current in Sec. 7). In the vicinity of the threshold, $V_2 < V < V_1$, this current exists only in the form of currents through the bound states and therefore it is completely converted into a supercurrent far away from the junction. At larger voltages, $V > V_1$, the side band $n=1$ extends outside the energy gap (see Fig. 8a), which also makes the current I_2 partially consist of contributions from extended states. The explicit expression for the second-order current is

$$I_2 = \frac{4e\Delta^3\lambda^2}{\pi R}\int_\Delta^{2eV-\Delta} dE \frac{|E_2|}{\xi\xi_2|\xi_1|^2} \times \cosh\Gamma_1\left(\frac{e^{-\gamma_0+\Gamma_1}}{P_2} + \frac{e^{\gamma_0-\Gamma_1}}{\bar{P}_2}\right). \qquad (9.7)$$

Omitting the λ-dependence of P_2 in Eq. (9.7), we obtain the two-particle tunnel current of Schrieffer and Wilkins.[42,57] To keep the singular terms in P_2 one has to truncate the continued fractions in Eq. (5.25) assuming $Z_{-1} = Z_3 = 1$, which yields

$$P_2 \approx |(1+\lambda a_{-1}^- a_0^-)(1+\lambda a_1^- a_2^-) + \lambda a_0^+ a_1^+ (1+\lambda a_2^+ a_3^+)|^2. \qquad (9.8)$$

The threshold singularity results from the small product $\xi\xi_2$ in the denominator of Eq. (9.7). However, in Eq. (9.8) there are no singular terms proportional to $a_0 a_2$ among the terms linear in λ. Such terms are quadratic in λ and they provide, along with the terms λa_0 and λa_2, the width of the onset: $e(V - V_2) \sim \lambda^2\Delta$. This onset is sharper than the onset of the current I_1.

The threshold singularity in the current I_2 is typical of all higher-order currents $n > 1$. The appearance of the first side band outside the energy gap at $V = V_1$ is manifested through a spike in the current I_2. Indeed, if $V \approx V_1$, the nodes of ξ_1 overlap the nodes of ξ and ξ_2 at the lower ($E = \Delta$) and the upper ($E = 3\Delta$) limits of integration in Eq. (9.7), respectively (see Fig. 8a). This singularity yields an increase of the current I_2 when the voltage approaches V_1,

$$I_2 \sim e\Delta\lambda^2\left(\frac{\Delta}{e(V_1 - V)}\right)^{1/2}.$$

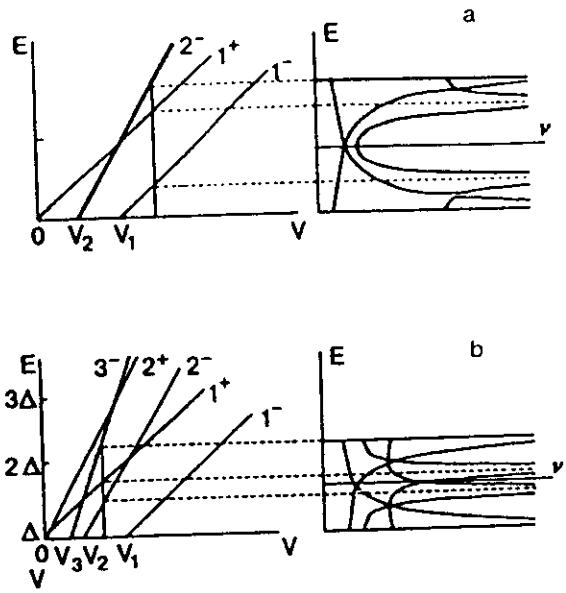

FIG. 8. a) Density of states $\nu(E) = |E_n/\xi_n|$ of the side bands and E_0, E_1, and E_2 at applied voltage $V > V_1$ (right), position of singularities of the side-band density of states plotted as function of the applied voltage for the current I_2 (left), $1^\pm: E_1 = \pm\Delta$, $2^-: E_2 = -\Delta$. b) Density of states of the side bands E_0, E_1, E_2, and E_3 at applied voltage $V_2 < V < V_1$ (right), position of singularities of the side-band density of states plotted as a function of the applied voltage for the current I_3 (left), $1^\pm: E_1 = \pm\Delta$, $2^\pm: E_2 = \pm\Delta$, $3^-: E_3 = -\Delta$.

Regularization of the integral, which is provided by the singular terms $\lambda a_1 a_0$ and $\lambda a_1 a_2$ in Eq. (9.8) at the lower and the upper integration limits, respectively, yields

$$\frac{I_2(V_1)}{I_2(V_2)} \sim \frac{1}{\sqrt{\lambda}}.$$

Further analysis shows that the current reaches a maximum value slightly above $V = V_1$, after which it rapidly decreases (see Fig. 9). At voltages $V > V_1$ the singular point $\xi_1 = 0$ remains within the integration region, which increases the current by a logarithmic factor in comparison with the value of the current near the threshold V_2,

$$I_2(V > V_1) \sim \frac{e\Delta\lambda^2 \ln\lambda}{R}. \qquad (9.9)$$

At large voltage $V \gg V_1$ the current I_2 forms the excess current [Eq. (7.10)]. It is interesting to note that in this limit the logarithmic factor is compensated for by the current I_1 [Eq. (8.9)], which yields the λ^2-dependence of the excess current.

The third-order current I_3 at voltages close to the threshold V_3 results from the combination of one-particle tunneling into the side band $n=3$ and excitation of the transmitted Andreev bound states of the side band $n=1$ (Fig. 7c). The probabilities of these two processes are related as 1:2 at threshold [Eq. (8.7)]. A gradual emergence of the bound states of the side bands $n=1$ and 2 outside the energy gap at $V = V_2$ and $V = V_1$ (Fig. 8b) gives rise to the current peaks. The current I_3 has the explicit form:

$$I_3=\frac{2e\Delta^5\lambda^3}{\pi R}\int_{\Delta}^{3eV-\Delta}dE\,\frac{|E_3|}{\xi\xi_3|\xi_1\xi_2|^2}$$
$$\times\left[\frac{e^{\gamma_0}(1+2\cosh\Gamma_1 e^{-\Gamma_1+2\Gamma_2})}{P_3}\right.$$
$$\left.+\frac{e^{-\gamma_0}(1+2\cosh\Gamma_1 e^{\Gamma_1-2\Gamma_2})}{\bar{P}_3}\right] \qquad (9.10)$$

with the regularization factor

$$P_3\approx|(1+\lambda a_{-1}^{-}a_0^{-})(1+\lambda a_1^{-}a_2^{-})(1+\lambda a_3^{-}a_4^{-})$$
$$+\lambda a_0^{+}a_1^{+}(1+\lambda a_2^{+}a_3^{+})|^2. \qquad (9.11)$$

The current peak at $V=V_2$ results from the overlap of nodes of ξ and ξ_2 at $E=\Delta$ and nodes of ξ_1 and ξ_3 at $E=2\Delta$, similarly to the peak of the current I_2. These singularities yield again an increase in the current inversely proportional to the square root of the departure from the voltage V_2: $I_3 - e\Delta^{3/2}\lambda^3/[e(V_2-V)]^{1/2}$. However, since the factor P_3 [Eq. (9.11)] contains neither the term $\lambda a_0 a_2$ nor the term $\lambda a_1 a_3$, regularization of the singularity is provided, e.g., at $E=\Delta$, by the terms λa_0 or λa_2, which gives rise to a more pronounced peak with magnitude

$$\frac{I_3(V_2)}{I_3(V_3)}\sim\frac{1}{\lambda}. \qquad (9.12)$$

We note that the magnitude of this peak is comparable to the magnitude of the onset of the current I_2. The second peak at $V=V_1$ results from the overlap of the nodes of ξ_2 and ξ_3 at $E=3\Delta$, which increases the current I_3 near the voltage $V=V_1$ which is inversely proportional to the first power of the distance to this voltage: $I_3\sim\lambda^3\Delta^2/(V_1-V)$. The divergence is regularized by the term $\lambda a_2 a_3$ in Eq. (9.11), which results in a peak of magnitude

$$\frac{I_3(V_1)}{I_3(V_3)}\sim\frac{1}{\lambda}. \qquad (9.13)$$

Thus the heights of the two peaks of the current I_3 are of the same order in λ, although the peak at $V\approx V_1$ is sharper.

In a similar way, all of the high-order currents in the vicinity of their thresholds are attributable either to the Andreev bound state currents (even n) or to a combination of Andreev bound state currents and the current of a single real excitation (odd n). The number of excited Andreev states is correspondingly $n/2$ or $(n-1)/2$. Singularities similar to the singularity of the current I_3 at the voltage $V\approx V_1$ exist in all high-order currents, where they cause even more pronounced current peaks because of the absence of terms $\lambda a_k a_{k+1}$ in the corresponding smearing functions P_n. Because of this property, the heights of such peaks exceed the threshold value of the corresponding current by two orders of λ: $(I_n)_{\max}\sim e\Delta\lambda^{n-2}/R$.

The above discussion reveals the current peaks to be essential features of the SGS of tunnel current in addition to the current onsets (Fig. 9) (these peaks are seen also in the numerical results of Refs. 34 and 39). It allows us to establish a general classification of singularities that cause peaks

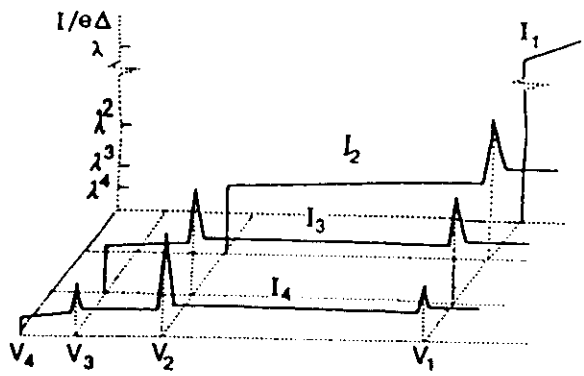

FIG. 9. Schematic diagram of the partial $I_n - V$ characteristics.

in partial currents I_n. They result from the overlap of singularities of the side band density of states. It is easy to see that the singularities of only two side bands can overlap. The condition of the overlap for mth and kth side bands have the form

$$E-keV=\Delta,\quad E-meV=-\Delta. \qquad (9.14)$$

This condition is met at voltages $eV=2\Delta/(m-k)$ for all integer $0\leq k<m\leq n$. The magnitude of the current peaks depends on whether the overlapping side bands are neighbors or not, and whether the side band index is inside or at the edge of the interval $(0,n)$.

I. $m-k=1, m=n$ or $k=0$: edge-type singularity, neighbor side bands. This type of singularity forms the peak of the current I_2 at the main threshold V_1. The magnitude of the current peak is $(I_2)_{\max}\sim e\Delta\sqrt{\lambda}/R$.

II. $m-k>1, m=n$ or $k=0$: edge-type singularity, non-neighbor side bands. This type of singularity forms the first peak of the current I_n, $n>2$ at voltage V_{n-1}. The magnitude of the current peak is $(I_n)_{\max}\sim e\Delta\lambda^{n-1}/R$.

III. $m-k=1, m<n, k>0$: internal singularity, neighbor side bands. This type of singularity forms the last peak of each current I_n, $n>2$ at voltage V_1. The magnitude of the current peak is $(I_n)_{\max}\sim e\Delta\lambda^{n-1}/R$.

IV. $m-k>1, m<n, k>0$: internal singularity, non-neighbor-side bands. This type of singularity forms all intermediate peaks of each current I_n, $n>3$. The magnitude of the current peaks are $(I_n)_{\max}\sim e\Delta\lambda^{n-2}/R$.

CONCLUSION

In this paper we have considered superconductive tunneling as a scattering problem within the framework of Bogolyubov-de Gennes (BdG) quantum mechanics. An essential aspect of this problem is that the scatterer consists not only of the potential of the tunnel barrier but also of the discontinuity of the phase of the order parameter. At equilibrium (zero bias, Josephson direct current) the scattering problem is *elastic*. The peculiar feature of the elastic scattering problem in short junctions, which is considered here, is that the balance of currents of the scattering modes is not violated: the supercurrent flows only through the superconducting bound states (for a more general discussion, see Ref. 48). In the presence of voltage bias the scattering is *inelastic*,

because the time dependence of the component of the scatterer is related to the superconducting phase difference. In general, the currents of all inelastic channels, taken collectively, constitute the components of the tunnel current that flows through the biased junction. The quasiparticle current corresponds to the incoherent part of the inelastic side band contributions, and the Josephson alternating current corresponds to the interference of the side band contributions.

There are three distinct components of the quasiparticle tunnel current at zero temperature: (i) the current of quasiparticles excited above the ground state, (ii) the current trough Andreev bound states converted to a supercurrent outside the junction, and (iii) the imbalance current of the ground state modes. At large bias voltage, $eV \gg 2\Delta$, the first component corresponds to a single particle current of the normal junction, while the other components cause excess current. When voltage is decreased, redistribution of current among the components gives rise to subharmonic gap structure (SGS) in the form of current onsets and current peaks. Within the voltage intervals $2\Delta/n < eV < 2\Delta/(n-1)$ with even n, the tunnel current consists entirely of currents through the Andreev bound states [component (ii); e.g., Fig. 7b]; the states of all side bands with odd indices smaller than n contribute to the current. If n is odd, a real excitation current of the side band n [component (i); e.g., Figs. 7a, and 7c] is also present in the tunnel current. Opening of new channels of tunneling of real excitations gives rise to current structures. Thus, SGS reveals the discrete nature of the side band spectrum. The structure becomes more pronounced with decreasing transparency of the junction.

Since each Andreev state provides transfer of one Cooper pair through the junction for every incident quasiparticle, n particles will tunnel in the interval $2\Delta/n < eV < 2\Delta/(n-1)$.

The participation of a large number of bound Andreev states in the current transport at low voltages is surprising: it appears to contradict the fact that subgap current diminishes at zero bias. After all, the probability of the scattering into side bands does not depend on the bias and is proportional to powers of D. This paradox can be solved by increasing the compensation of currents between the normal and Andreev channels in each side band with decreasing voltage, which gives the required voltage dependence of the total current.

ACKNOWLEDGMENT

This work was supported by the Swedish National Science Research Council (NFR), the Swedish National Board for Technical and Industrial Development (NUTEK), and the Swedish Royal Academy of Sciences (KVA).

APPENDIX A: BOUNDARY CONDITIONS

The quasiclassical boundary condition in Eqs. (2.8) and (2.9) has been derived in Ref. 31 by using the method of Ref. 21. Here we present simple arguments which lead to this boundary condition. We consider the more general case of asymmetric junction, using an asymmetric version of the Hamiltonian of Eq. (2.2) with the same restriction imposed on the length of the nonsuperconducting region, $L \ll \xi_0$. We include a contact potential difference in the potential $U(x)$, which implies that this potential may have nonvanishing asymptotic values at infinity: $U(-\infty) \neq U(\infty) \neq 0$. If the junction has more than one transverse transport mode, we assume that these modes are not mixed.

A one-dimensional quasiclassical wave function of a given transverse channel in the right electrode has the form [Eq. (2.6)],

$$\Psi_R(x,t) = \sum_\beta \frac{1}{\sqrt{v_R}} \exp\left(i\beta \int p_R dx\right) \times \exp(i\sigma_z \chi_R/2)\psi_R^\beta(x,t), \tag{A1}$$

with a similar expression for the left electrode. The quantities ψ_R^β are slowly varying two-component wave functions on the scale of $1/p_R$, where $p_R(x) = [2m_R(\mu - U_R - E_{\perp R}(x))]^{1/2}$. This equation is valid over the distance $x \gg 1/p_R$ from the junction, and in the spatial region $1/p_R \ll x \ll \xi_0$ the functions ψ_R^β are almost constant.

From another point of view, at large distance from the junction, $|x| \gg 1/p_{R,L}$, the function Ψ can be expressed in the form of a linear combination of the scattering states at the Fermi level,

$$\Psi = C_1\chi_1 + C_2\chi_2 \tag{A2}$$

$$\chi_1 = \begin{cases} (1/\sqrt{v_L})[e^{ip_L x} + re^{-ip_L x}], & x<0, \\ (1/\sqrt{v_R})de^{ip_R x}, & x>0, \end{cases} \tag{A3a}$$

$$\chi_2 = \begin{cases} (1/\sqrt{v_R})[e^{-ip_L x} + \tilde{r}e^{-ip_R x}], & x>0, \\ (1/\sqrt{v_L})\tilde{d}e^{-ip_L x}, & x<0. \end{cases} \tag{A3b}$$

Comparing Eqs. (A2) and (A3) with Eq. (A1) in the region $1/p_F \ll |x| \ll \xi_0$, we have

$$C_1 = e^{i\varphi_L/2}\psi_L^+, \quad C_2 = e^{i\varphi_R/2}\psi_R^-,$$

$$rC_1 + \tilde{d}C_2 = e^{i\varphi_L/2}\psi_L^-,$$

$$dC_1 + \tilde{r}C_2 = e^{i\varphi_R/2}\psi_R^+, \tag{A4}$$

which yields the boundary condition

$$\begin{pmatrix} \psi_L^- \\ \psi_R^+ \end{pmatrix} = \hat{V}\begin{pmatrix} \psi_L^+ \\ \psi_R^- \end{pmatrix}, \tag{A5}$$

with the matching matrix

$$\hat{V} = \begin{pmatrix} r & \tilde{d}e^{i(\varphi_R - \varphi_L)/2} \\ de^{i(\varphi_L - \varphi_R)/2} & \tilde{r} \end{pmatrix}, \tag{A6}$$

where $\varphi = \chi_R(0) - \chi_L(0)$. The matrix $\hat{V}$ satisfies the unitarity condition $\hat{V}\hat{V}^+ = 1$, provided by the relations among the normal electron scattering amplitudes in Eq. (A3) $\tilde{r} = -\tilde{d}(r/d)^*$, $|d|^2 = |\tilde{d}|^2 = D$, $|r|^2 = |\tilde{r}|^2 = R = 1 - D$.

APPENDIX B: BOUND STATE CURRENT

Equation (4.10) for the current of a single bound state can be derived directly[31] from the Bogolyubov-de Gennes equations (2.5) and (2.2). The derivation is valid for junctions with an arbitrary nonsuperconducting region between the superconducting electrodes. We assume for simplicity

that the phase of the order parameter [Eq. (2.3)] in the electrodes is constant and equal to $\pm\ \varphi/2$ in the right and left electrodes, respectively. Let $\Psi(\mathbf{r},E)$ be a normalized wave function of the Andreev bound state with energy E,

$$\hat{H}\Psi - E\Psi = 0, \quad \Psi(x = \pm\infty) = 0. \tag{B1}$$

The energy and the wave function of the bound state depend on the phase difference φ. Using the derivative with respect to φ in Eq. (B1) and a scalar product of the resulting equation with the function Ψ, we obtain

$$\int d^3r\left(\Psi, \frac{d}{d\varphi}(\hat{H} - E)\Psi\right) = 0, \tag{B2}$$

where the brackets denote a scalar product in the electron-hole space, similar to Eq. (3.8). In this equation the derivative of the Hamiltonian has the form

$$\frac{d\hat{H}}{d\varphi} = \frac{d\hat{\Delta}}{d\varphi} = \frac{i\ \mathrm{sign}\ x}{2}\sigma_z\hat{\Delta}, \tag{B3}$$

in accordance with Eqs. (2.2) and (2.3). Substituting relation (B3) into Eq. (B2) and taking into account that the function Ψ is normalized, we obtain

$$\frac{dE}{d\varphi} = \int d^3r\left(\Psi, \frac{d\hat{\Delta}}{d\varphi}\Psi\right). \tag{B4}$$

The continuity equation for the charge current,

$$I(x,E) = \frac{e}{2m}(\hat{p}_x - \hat{p}'_x)\int d^2r_\perp(\Psi(x'),\Psi(x))_{x=x'}, \tag{B5}$$

in accordance with Eq. (B1), has the form

$$i\frac{d}{dx}I(x,E) = e\int d^2r_\perp(\Psi(x),[\sigma_z,\hat{\Delta}]\Psi(x)). \tag{B6}$$

Substituting relation (B3) into Eq. (B6) and integrating this equation over the entire x axis, we obtain

$$I(0,E) = 2e\int d^3r\left(\Psi, \frac{d\hat{\Delta}}{d\varphi}\Psi\right). \tag{B7}$$

In Eq. (B7) the current at infinity drops out because of decay of the bound state wave function, $I(\pm\infty) = 0$. The current $I(0)$ is formally taken in the middle of the junction; however, the current has the same value in the whole nonsuperconducting region, according to the conservation equation (B6). Comparison of Eqs. (B4) and (B7) finally yields

$$I(E) = 2e\frac{dE}{d\varphi}. \tag{B8}$$

[1] J. Bardeen, Phys. Rev. Lett. **6**, 57 (1961).
[2] A. Barone and G. Paterno, Physics and Applications of the Josephson Effect, Wiley, New York (1982).
[3] C. L. Foden, R. Rando, A. van Dordrecht, A. Peacock, J. Lumley, and C. Pereira, Phys. Rev. B**47**, 3316 (1993).
[4] R. Cristiano, I. Frenzio, R. Monaco, C. Nappi, and S. Pagano, Phys. Rev. B**49**, 429 (1994).
[5] A. W. Kleinsasser, R. E. Miller, W. H. Mallison, and G. B. Arnold, Phys. Rev. Lett. **72**, 1738 (1994).
[6] H. Takayanagi and T. Kawakami, Phys. Rev. Lett. **54**, 2449 (1985).
[7] A. Frydman and Z. Ovadyahu, Solid State Commun. **95**, 79 (1995).
[8] N. van der Post, E. T. Peters, I. K. Yanson, and J. M. van Ruitenbeek, Phys. Rev. Lett. **73**, 2611 (1994).
[9] H. Takayanagi, T. Akazaki, and J. Nitta, Phys. Rev. Lett. **75**, 3533 (1995).
[10] W. Haberkorn, H. Knauer, and S. Richter, Phys. Status Solidi **47**, K161 (1978).
[11] A. V. Zaitsev, Zh. Éksp. Teor. Fiz. **86**, 1742 (1983) [Sov. Phys. JETP **59**, 1015 (1984)].
[12] G. B. Arnold, J. Low Temp. Phys. **59**, 143 (1985).
[13] L. G. Aslamasov and B. Fistul', Zh. Éksp. Teor. Fiz. **83**, 1170 (1982) [Sov. Phys. JETP **56**, 666 (1982)].
[14] C. Ishii, Prog. Theor. Phys. **44**, 1525 (1970).
[15] A. V. Svidzinsky, T. N. Anzygina, and E. N. Bratus', J. Low Temp. Phys. **10**, 131 (1973).
[16] I. O. Kulik and A. N. Omel'yanchuk, Fiz. Nisk. Temp. **3**, 945 (1977); **4**, 296 (1978) [Sov. J. Low Temp. Phys. **3**, 459 (1977); **4**, 142 (1978)].
[17] S. N. Artemenko, A. F. Volkov, and A. V. Zaitsev, Zh. Éksp. Teor. Fiz. **76**, 1816 (1979) [Sov. Phys. JETP **49**, 924 (1979)].
[18] I. O. Kulik, Zh. Éksp. Teor. Fiz. **57**, 1745 (1969) [Sov. Phys. JETP **30**, 944 (1970)].
[19] J. Bardeen and J. L. Jonson, Phys. Rev. B**5**, 72 (1972).
[20] P. G. de Gennes, Superconductivity of Metals and Alloys, Addison-Wesley, New York (1989).
[21] A. V. Svidzinsky, Spatial Inhomogeneity Problems in the Theory of Superconductivity, Nauka, Moscow (1982) (in Russian).
[22] I. F. Itskovich and R. I. Shekhter, Fiz. Nizk. Temp. **7**, 863 (1981) [Sov. J. Low Temp. Phys. **7**, 418 (1981)].
[23] G. E. Blonder, T. M. Klapwijk, and M. Tinkham, Phys. Rev. B**25**, 4515 (1982).
[24] C. W. J. Beenakker and H. van Houten, Phys. Rev. Lett. **66**, 3056 (1991).
[25] P. F. Bagwell, Phys. Rev. B**46**, 12573 (1992).
[26] C. W. J. Beenakker, Phys. Rev. Lett. **67**, 3836 (1991).
[27] M. Hurd and G. Wendin, Phys. Rev. B**49**, 15258 (1994).
[28] L. Y. Gorelik, V. S. Shumeiko, R. I. Shekhter, G. Wendin, and M. Jonson, Phys. Rev. Lett. **75**, 1162 (1995).
[29] A. Furusaki and M. Tsukada, Physica B**165–166**, 967 (1990); Phys. Rev. B**43**, 10164 (1991).
[30] C. W. J. Beenakker and H. van Houten, in Single Electron Tunneling and Mesoscopic Devices, Springer, Berlin (1991).
[31] V. S. Shumeiko, E. N. Bratus', and G. Wendin, Phys. Rev. B**48**, 13129 (1993).
[32] T. M. Klapwijk, G. E. Blonder, and M. Tinkham, Physica B+C **109–110**, 1657 (1982).
[33] E. N. Bratus', V. S. Shumeiko, and G. Wendin, Phys. Rev. Lett. **74**, 2110 (1995).
[34] D. Averin and A. Bardas, Phys. Rev. Lett. **75**, 1831 (1995).
[35] B. J. van Wees, H. van Houten, C. W. J. Beenakker, J. G. Williamson, L. P. Kouwenhoven, D. van der Marel, and C. T. Foxon, Phys. Rev. Lett. **60**, 848 (1988).
[36] R. Landauer, IBM J. Res. Dev. **1**, 223 (1957).
[37] S. V. Kuplevakhskii and I. I. Fal'ko, Fiz. Nizk. Temp. **17**, 961 (1991) [Sov. J. Low Temp. Phys. **17**, 501 (1991)].
[38] B. D. Josephson, Adv. Phys. **14**, 419 (1965).
[39] G. B. Arnold, J. Low Temp. Phys. **68**, 1 (1987).
[40] A. D. Stone, M. Ya. Azbel, and P. A. Lee, Phys. Rev. B**31**, 1707 (1985).
[41] P. F. Bagwell and R. K. Lake, Phys. Rev. B**46**, 15329 (1992).
[42] J. R. Schrieffer and J. W. Wilkins, Phys. Rev. Lett. **10**, 17 (1963).
[43] L. I. Glazman, G. B. Lesovik, D. E. Khmel'nitskii, and R. I. Shekhter, Pis'ma Zh. Éksp. Teor. Fiz. **48**, 218 (1988) [JETP Lett. **48**, 238 (1988)].
[44] J. Bardeen, R. Kummel, A. E. Jacobs, and L. Tewordt, Phys. Rev. **187**, 556 (1969).
[45] I. O. Kulik, R. I. Shekhter, and A. N. Omel'yanchouk, Solid State Commun. **23**, 301 (1977).
[46] M. Yu. Kupriyanov and V. F. Lukichev, Zh. Éksp. Teor. Fiz. **94**, 139 (1988) [Sov. Phys. JETP **67**, 1163 (1988)].
[47] I. A. Devyatov and M. Yu. Kupriyanov, Pis'ma Zh. Éksp. Teor. Fiz. **59**, 187 (1994) [JETP Lett. **59**, 200 (1994)].
[48] G. Wendin and V. S. Shumeiko, Phys. Rev. B**53**, R6006 (1996).
[49] A. F. Andreev, Zh. Éksp. Teor. Fiz. **46**, 1823 (1964) [Sov. Phys. JETP **19**, 1228 (1964)].
[50] J. R. Schrieffer, Theory of Superconductivity, Benjamin, New York (1964).
[51] V. P. Galaiko, Zh. Éksp. Teor. Fiz. **61**, 382 (1971) [Sov. Phys. JETP **34**, 203 (1972)].

[52]The contribution from the continuum does not vanish if there is imbalance of populations of electron-like and hole-like branches of the quasiparticle spectrum in one of the electrodes.
[53]V. Ambegaokar and A. Baratoff, Phys. Rev. Lett. **10**, 468 (1963).
[54]N. R. Werthamer, Phys. Rev. **147**, 255 (1966).
[55]E. N. Bratus' and V. S. Shumeiko, Fiz. Tverd. Tela **21**, 2821 (1979) [Sov. Phys. Solid State **21**, 1506 (1979)].
[56]B. N. Taylor and E. Burstein, Phys. Rev. Lett. **10**, 14 (1963).
[57]J. W. Wilkins, in Tunneling Phenomena in Solids, Plenum, New York (1963).
[58]L. E. Hasselberg, J. Phys. F**3**, 1438 (1973); L. E. Hasselberg, M. T. Levinsen, and M. R. Samuelsen, Phys. Rev. B**9** 3757 (1974).
[59]E. L. Wolf, Principles of Electron Tunnel Spectroscopy, Oxford University, New York (1985).
[60]M. H. Cohen, L. H. Fallcov, and J. C. Phillips, Phys. Rev. Lett. **8**, 316 (1962).
[61]L. Y. Gorelik, unpublished.

This article was published in English in the original Russian journal. It was edited by S. J. Amoretty.

dc-current transport and ac Josephson effect in quantum junctions at low voltage

E. N. Bratus', V. S. Shumeiko, and E. V. Bezuglyi
Department of Applied Physics, Chalmers University of Technology and Göteborg University, S-41296 Göteborg, Sweden and B. Verkin Institute for Low Temperature Physics and Engineering, 47 Lenin Avenue, 310164 Kharkov, Ukraine

G. Wendin
Department of Applied Physics, Chalmers University of Technology and Göteborg University, S-41296 Göteborg, Sweden

(Received 30 December 1996)

Multiple Andreev scattering in single-mode superconducting junctions with arbitrary normal electron transparency $0<D<1$ is studied in the limit of low applied voltage $eV\ll\Delta$. A quasiclassical approach is developed for investigation of the dense lattice of inelastic sidebands associated with multiple Andreev scattering, which gives a global description of inelastic-scattering amplitudes and spectral distribution of the current. The crossover from the contact to the tunnel regime is investigated for the dc current and ac Josephson current as function of junction transparency and applied voltage. A mesoscopic interference effect in junctions with intermediate transparency is discussed. This effect shows up in oscillating features of the current of thermal excitations. [S0163-1829(97)06418-7]

I. INTRODUCTION

During the last 15 years significant effort has been directed towards understanding the physical processes in biased superconducting junctions at applied voltages smaller than the gap value, $eV<2\Delta$ (Refs. 1–7). The interest in the problem is due to the fact that single-particle current transport at zero temperature is entirely blocked at subgap voltage,[8] and that the current has multiparticle origin.[9] Considerable subgap current is systematically observed in experiment, especially in transparent junctions, manifesting a pronounced subharmonic gap structure.[10–14] The multiparticle mechanism of subgap transport has been found to be closely related to Andreev processes of electron-hole conversions in the junction[1,4] and to the formation of Andreev bound states within the superconducting energy gap.[15]

The progress during the last few years has been due to careful investigations of quantum point contacts. Such structures are available in real experiments on break-junction devices[16,17] and on gated superconductor-semiconductor devices.[18]

In quantum point contacts the problem of subgap current is presented in a refined form. The small size of the junction on the scale of the phase-breaking length, and the separation of transverse electron modes, makes it possible to treat the current through each separate mode in the spirit of the scattering theory approach.[19,20] The total current through the junction then results from imbalanced currents of quasiparticle scattering states originating from the left and right superconducting electrodes. Quasiparticle scattering in biased superconducting junctions is inelastic because of nonstationary behavior of the superconducting phase difference at the junction. It therefore involves an infinite set of sidebands in the spectrum of scattered waves with energies shifted by an integer number of quanta eV (Ref. 15). Furthermore, some of the sideband states are created within the superconducting gap in the form of Andreev bound states. These states carry current which is converted into supercurrent outside the junction, providing transmission of Cooper pairs through the junction. Thus, a dc pair current necessarily accompanies the single-particle current of real excitations.

Cancellation of the currents of different inelastic channels, including normal and Andreev current components, is extremely nontrivial. Perturbative analysis of the current in junctions with low normal electron transparency $D\ll 1$ has shown[15,21] that the normal and Andreev components of the pair current are balanced in a such way that the pair current experiences rapid changes (onsets and spikes) near voltages $eV=2\Delta/n$. Together with the onsets of the single-particle current this yields the steplike subharmonic gap structure, as shown in Fig. 1. The theoretical results perfectly fit break-junction experimental data without fitting parameters.[22] The subharmonic gap structure in quantum junctions with arbitrary transparency has been numerically calculated using different methods in Refs. 4,23,24.

At low applied voltages, $eV\ll\Delta$, the number of inelastic sidebands increases without limit. However, in junctions with small transmissivity, $D\ll 1$, the dc current decays exponentially with decreasing the applied voltage,[25] Fig. 1. Very different properties of the dc current have been revealed in the opposite limit of fully transparent junctions, $D=1$. In this limit, the dc current appears as the average of the time-dependent current associated with adiabatic oscillations of the Andreev bound states, which approaches constant magnitude at low applied voltage,[23] giving rise to a zero-bias peak of the junction conductance.[7,24]

In this paper we analyze the current through superconducting junctions at low applied voltage $eV\ll\Delta$ in the whole range of junction transparency $0<D<1$. Taking advantage of the high spectral density of the sideband lattice, we develop a quasiclassical description of the spectral distribution of the inelastic-scattering amplitudes. This allows us to investigate the global structure of the inelastic scattering amplitudes and the distribution of current among different inelastic channels.

The structure of the paper is the following: in Sec. II we

0163-1829/97/55(18)/12666(12)/$10.00

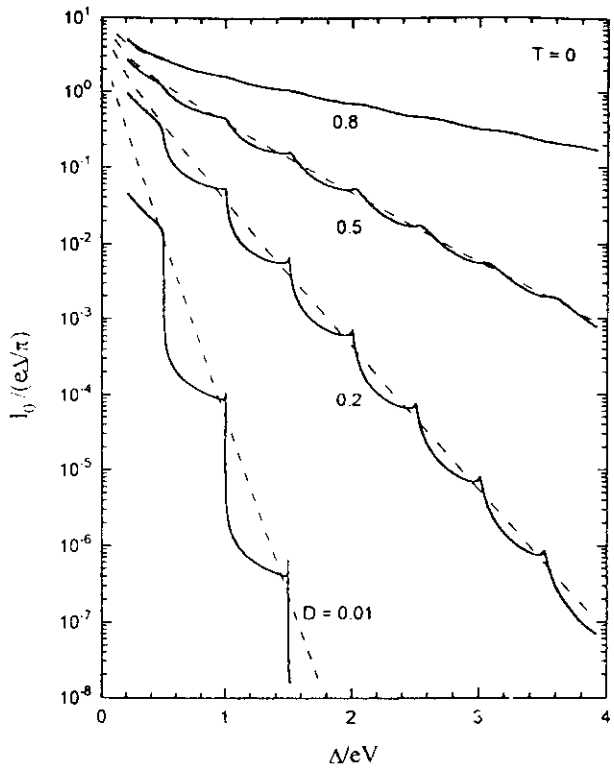

FIG. 1. The subharmonic gap structure of a biased single-mode quantum point contact at zero temperature and at different junction transparencies: $D = 0.01, 0.2, 0.5, 0.8$. The solid lines represent the result of a numerical calculation based on the exact recurrences in Eqs. (3.2a), (3.2b); dashed lines are the analytical result of quasiclassical theory, Eqs. (4.4), (4.5), (4.9).

derive equations for inelastic-scattering amplitudes, while Sec. III is devoted to construction of quasiclassical solutions of these equations. The dc current is calculated in Sec. IV and the ac current is finally discussed in Sec. V.

II. EQUATIONS FOR SCATTERING AMPLITUDES

We consider a superconducting quantum constriction with a local scatterer in the neck (Fig. 2). We assume here that the junction is symmetric, that the constriction is smooth on the scale of the Fermi wavelength, and that there is only a single transport mode. We consider quasiparticle scattering by the junction using the Bogoliubov–de Gennes (BdG) equation[27]

$$i\dot{\Psi}(t)=\hat{H}\Psi(t) \tag{2.1}$$

with the Hamiltonian

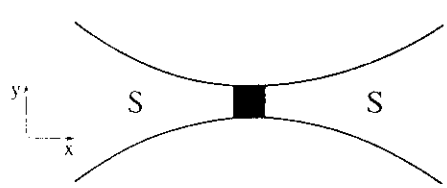

FIG. 2. One-channel adiabatic superconducting constriction. The dark region represents the scatterer with normal electron transparency $0<D<1$.

$$\hat{H}=\left[\frac{[\hat{\vec{p}}-\sigma_z e\vec{A}(\vec{r},t)]^2}{2m}+V(\vec{r})-\mu\right]\sigma_z + [U(x)+e\varphi(\vec{r},t)]\sigma_z+\hat{\Delta}(\vec{r},t). \tag{2.2}$$

In Eq. (2.2), $V(\vec{r})$ is the potential defining the constriction, $U(x)$ is the potential of the scatterer, $\vec{A}(\vec{r},t)$ and $\varphi(\vec{r},t)$ are electromagnetic potentials, and $\hat{\Delta}(\vec{r},t)$ is the superconducting order parameter given by the matrix

$$\hat{\Delta}=\begin{pmatrix} 0 & \Delta e^{i\chi/2} \\ \Delta e^{-i\chi/2} & 0 \end{pmatrix}. \tag{2.3}$$

σ_z is the Pauli matrix, and the choice of units corresponds to $c=\hbar=1$.

Due to the adiabatic geometry of the junction,[26] we may use the quasiclassical wave functions far from the scatterer,

$$\Psi(\vec{r},t)=\sum_{\beta}\psi_{\perp}(\vec{r}_{\perp},x)\frac{1}{\sqrt{v}}e^{i\beta\int p\,dx}\psi^{\beta}(x,t), \tag{2.4}$$

where $\psi_{\perp}(x),\psi^{\beta}(x)$ are slowly varying functions, $\psi_{\perp}$ is the normalized wave function of the transverse mode, $p=\sqrt{2m(\mu-E_{\perp})}$ is the longitudinal momentum of the quasiclassical electron, $v=p/m$, and $\beta=\pm$ indicates the direction of electron motion. We will also explicitly separate out the phase $\chi(\vec{r},t)$ of the superconducting order parameter $\hat{\Delta}$ in Eq. (2.3) by means of a gauge transformation

$$\psi^{\beta}\to e^{i\sigma_z\chi/2}\psi^{\beta}, \tag{2.5}$$

and introduce a superfluid momentum $\vec{p}_s=\nabla\chi/2-e\vec{A}$ and a gauge-invariant electric potential $\Phi=\dot{\chi}/2+e\varphi$. The coefficients ψ^{β} in Eq. (2.4) then obey the reduced BdG equation:

$$i\dot{\psi}^{\beta}_{L,R}=(\beta v\hat{p}\sigma_z+\Phi_{L,R}\sigma_z+vp_{sL,R}+\Delta\sigma_x)\psi^{\beta}_{L,R} \tag{2.6}$$

in the left (L) and the right (R) electrodes. Within such an approximation, the local scatterer in the neck of the constriction imposes a boundary condition to Eq. (2.6), which is determined by the normal electron-scattering amplitudes d and r ($|d|^2+|r|^2=D+R=1$, $r/d=-r^*/d^*$). If the scattering amplitudes are energy-independent near the Fermi level, the boundary condition has the form[21,28]

$$\begin{pmatrix}\psi^{-}_{L}\\ \psi^{+}_{R}\end{pmatrix}=\begin{pmatrix} r & de^{i\sigma_z\phi/2}\\ de^{-i\sigma_z\phi/2} & r\end{pmatrix}\begin{pmatrix}\psi^{+}_{L}\\ \psi^{-}_{R}\end{pmatrix}_{x=0}, \tag{2.7}$$

where ϕ is the gauge-invariant difference of the superconducting phases of the right and left electrodes: $\phi(t)=\chi_R(0,t)-\chi_L(0,t)$.

In the point-contact geometry, the effect of spreading out of the current gives rise to a negligibly small spatial deviation of the order parameter Δ from constant magnitude,[29] $\Delta=\text{const}$. For the same reason, practically the whole applied voltage drop V occurs at the junction,[30] $\varphi_L-\varphi_R=V$. Neglecting effects of penetration of the electromagnetic field into the superconductor, we omit the potentials p_s and Φ

from Eq. (2.6), $p_s=\Phi=0$. The relation $\Phi=0$ yields the Josephson relation between the phase difference and the applied voltage, $\dot{\phi}=2eV$.

In view of the time dependence of the boundary condition in Eq. (2.7), the scattering states are to be constructed from the eigenstates of Eq. (2.6) for different energies $E_n=E+neV$, shifted with respect to the energy E of the incoming wave by an integer multiple of eV, $-\infty<n<\infty$. The wave functions of the scattering states, calculated at the midpoint of the junction ($x=0$), have the form

$$\begin{pmatrix}\psi_L^-\\ \psi_R^+\end{pmatrix}_{jE}=\begin{pmatrix}\delta_{j,1}\\ \delta_{j,2}\end{pmatrix}\frac{u_E}{\sqrt{E}}e^{-iEt}+\sum_n\begin{pmatrix}a\\ b\end{pmatrix}_{jn}u_n^+e^{-iE_nt}, \quad (2.8)$$

$$\begin{pmatrix}\psi_L^+\\ \psi_R^-\end{pmatrix}_{jE}=\begin{pmatrix}\delta_{j,3}\\ \delta_{j,4}\end{pmatrix}\frac{u_E^-}{\sqrt{E}}e^{iEt}+\sum_n\begin{pmatrix}c\\ f\end{pmatrix}_{jn}u_n^-e^{iE_nt},$$

where $j=1-4$ labels scattering states having the same incoming energy E. In Eqs. (2.8) u_n is solution of the homogeneous BdG equation,

$$u_n^{\pm}=\frac{1}{\sqrt{2}}\begin{pmatrix}e^{\pm\gamma_n/2}\\ \sigma_n e^{\mp\gamma_n/2}\end{pmatrix}, \quad (2.9)$$

$$e^{\gamma_n}=\frac{|E_n|+\xi_n}{\Delta}, \quad \sigma_n=\mathrm{sgn}(E_n),$$

$$\xi_n=\begin{cases}\sqrt{E_n^2-\Delta^2}, & |E_n|>\Delta\\ i\sigma_n\sqrt{\Delta^2-E_n^2}, & |E_n|<\Delta\end{cases}$$

Combination of Eqs. (2.7)–(2.9) yields equations for the scattering amplitudes which reduce to a closed set of recurrences for the transmission amplitudes. For example, for a holelike quasiparticle incoming from the left ($j=1$), the recurrences read

$$\begin{pmatrix}b_{n+1}\\ f_{n+1}\end{pmatrix}=\hat{M}_n\begin{pmatrix}b_{n-1}\\ f_{n-1}\end{pmatrix}-\frac{2e^{3\gamma_0/2}\sinh\gamma_0}{d\sqrt{E}}\begin{pmatrix}re^{-\gamma_1/2}\\ e^{\gamma_1/2}\end{pmatrix}\delta_{n,0}, \quad (2.10)$$

where the matrix $\hat{M}_n$ has the form

$$\hat{M}_n=\sigma_n\sigma_{n-1}\begin{pmatrix}(e^{\gamma_n}-(2/D)\sinh\gamma_n)e^{(\gamma_{n+1}+\gamma_{n-1})/2} & (2r/D)\sinh\gamma_n e^{(\gamma_{n+1}-\gamma_{n-1})/2}\\ (-2r^*/D)\sinh\gamma_n e^{(\gamma_{n+1}-\gamma_{n-1})/2} & (e^{-\gamma_n}+(2/D)\sinh\gamma_n)e^{(\gamma_{n+1}+\gamma_{n-1})/2}\end{pmatrix}, \quad (2.11)$$

and where

$$\mathrm{Det}\hat{M}_n=1.$$

The transmission amplitudes of the other scattering states $j=2-4$ satisfy similar equations and are related to the solution of equations (2.10), (2.11) through the symmetry relations

$$\begin{pmatrix}b_{3n}\\ f_{3n}\end{pmatrix}(\gamma,r,d)=\begin{pmatrix}f_n\\ b_n\end{pmatrix}(-\gamma,r^*,d^*), \quad (2.12a)$$

$$\begin{pmatrix}c_{2n}\\ a_{2n}\end{pmatrix}(\gamma)=\sigma_0\sigma_n\begin{pmatrix}f_n\\ b_n\end{pmatrix}(-\gamma). \quad (2.12b)$$

The relation between the amplitudes of the scattering states $j=4$ and $j=2$ is similar to Eq. (2.12a).

The charge current associated with a single scattering state is given by the standard quantum-mechanical formula

$$I_{jE}(x,t)=\frac{e}{2m}\left\{(\hat{p}-\hat{p}')\int d^2r_\perp(\Psi(\vec{r}',t),\Psi(\vec{r},t))\right\}_{\vec{r}=\vec{r}'}. \quad (2.13)$$

The brackets in Eq. (2.13) denote a scalar product in electron-hole space. Eq. (2.13) is a particular form of a general equation for the charge current in nonequilibrium superconductors derived, e.g., in Ref. 31. In the quasiclassical approximation of Eq. (2.4) the current (2.13), calculated at the junction has form

$$I_{jE}(\pm 0,t)=e\sum_\beta\beta|\psi_{jE}^\beta(\pm 0,t)|^2. \quad (2.14)$$

The current in Eq. (2.14) can be calculated at either side of the junction; identity of the both expressions is guaranteed by the unitarity of the matching matrix in Eq. (2.7).

The wave function $\Psi(t)$ in Eq. (2.1) describes evolution in time of a quasiparticle state which originates from an eigenstate of the homogeneous BdG equation. According to the assumption of local equilibrium in the electrodes, a quasiparticle distribution among the eigenstates corresponds to the Fermi distribution. The total current results from Eq. (2.14) after summation over all quantum numbers of the incoming states, $|E|>\Delta$, $j=1-4$, with account of the Fermi filling factors. Expressing partial transmitted currents of individual scattering states in Eq. (2.14) through the scattering amplitudes, and making use of relations (2.12) and the symmetry relations

$$b_n(-E,\gamma,r,d)=\sigma_n b_{-n}^*(E,-\gamma,r^*,d^*), \quad (2.15)$$

$$f_n(-E,\gamma,r,d)=\sigma_n f_{-n}^*(E,-\gamma,r^*,d^*),$$

we finally arrive at an equation for the total current,

$$I(t)=\frac{e}{\pi N}\sum_{n=-\infty}^{\infty}e^{i2neVt}\int_\Delta^\infty\frac{dE\,E}{\xi}\tanh(E/2T)\sum_{n=odd}K_{n+2N,n}, \quad (2.16)$$

where

$$K_{nm}=(1/2)(1+\sigma_n\sigma_m)\{[(u_n^-,u_m^-)f_n^*f_m-(u_n^+,u_m^+)b_n^*b_m]-[\gamma\rightarrow-\gamma]\}. \quad (2.17)$$

When deriving Eq. (2.17) we have taken into account the fact that the products of scattering amplitudes $f_n^*f_m$ and $b_n^*b_m$ depend on the scattering probabilities D and R rather than on the scattering amplitudes d and r [see below Eqs. (3.2), (3.3)].

The form of the recurrences in Eq. (2.10), together with equation Eq. (2.17) for the current spectral density, allows us to make an important observation. The matrix elements in Eq. (2.11) are related, for all n, as

$$M_{11}(\gamma)=M_{22}(-\gamma), \quad M_{12}(\gamma,r)=M_{21}(-\gamma,r^*). \quad (2.18)$$

Within the superconducting gap the quantities γ_n in Eq. (2.9) are imaginary, and the symmetry relations in Eq. (2.18) take the form

$$\hat{M}_n\sigma_z\hat{M}_n^\dagger=\sigma_z. \quad (2.19)$$

This generates a conservation law

$$|b_n|^2-|f_n|^2=\text{const}, \quad |E_n|<\Delta, \quad (2.20)$$

which imposes a constant distribution of the time-independent current ($N=0$) of *each scattering state* among the Andreev bound states.

III. QUASICLASSICAL SOLUTIONS

Although a formal solution of the homogeneous equation in Eq. (2.10) is easily obtained:

$$\begin{pmatrix} b_{2n+1} \\ f_{2n+1} \end{pmatrix}=\prod_{k=1}^{k=n}\hat{M}_{2k}\begin{pmatrix} b_1 \\ f_1 \end{pmatrix}, \quad (3.1)$$

this is not very helpful because in junctions with arbitrary transparency $D\neq1$, the matrices $\hat{M}_n$ do not commute and the product in Eq. (3.1) cannot be calculated analytically. The exception is a perfect constriction, $R=0$, where the matrices $\hat{M}_n$ are diagonal and explicit calculation of the scattering amplitude is possible.[23] In the limit of low voltage, $eV/\Delta\ll1$, the matrices $\hat{M}_n$ change slowly with n and nearly commute if their indices are close to each other, which allows application of the two-scale expansion technique for approximate calculation of the product.

In this paper we will use another way of approximate calculation. We split the matrix equation (2.10) into two independent second-order difference equations

$$A_n^+f_{n+2}+A_n^-f_{n-2}+A_nf_n=-\frac{2\sinh\gamma_n}{d\sqrt{E/\Delta}}(e^{-(\gamma_0+\gamma_1)/2}\delta_{n,1}-\sigma_0\sigma_{-1}e^{(\gamma_0+\gamma_{-1})/2}\delta_{n,-1}), \quad (3.2a)$$

$$\bar{A}_n^+b_{n+2}+\bar{A}_n^-b_{n-2}+\bar{A}_nb_n=\frac{2r\sinh\gamma_n}{d\sqrt{E/\Delta}}(e^{(\gamma_1-\gamma_0)/2}\delta_{n,1}-\sigma_0\sigma_{-1}e^{(\gamma_0-\gamma_{-1})/2}\delta_{n,-1}), \quad (3.2b)$$

where the coefficients are given by

$$A_n^+=-\sigma_n\sigma_{n+1}e^{(\gamma_n-\gamma_{n+2})/2}\frac{\sinh\gamma_n}{\sinh\gamma_{n+1}},$$

$$A_n^-=-\sigma_{n-1}\sigma_{n-2}e^{-(\gamma_n+\gamma_{n-2})/2}\frac{\sinh\gamma_n}{\sinh\gamma_{n-1}}, \quad (3.3)$$

$$A_n=\frac{4}{D}\sinh^2\gamma_n+e^{\gamma_n-\gamma_{n+1}}\frac{\sinh\gamma_n}{\sinh\gamma_{n+1}}+e^{-\gamma_n+\gamma_{n-1}}\frac{\sinh\gamma_n}{\sinh\gamma_{n-1}},$$

$$\bar{A}(\gamma)=A(-\gamma).$$

Then, taking advantage of the short period of the sideband lattice and the slow variation of the coefficients in Eqs. (3.3), we transform the difference equations (3.2) into differential equations and apply the familiar technique of the quasiclassical approximation. Such a method allows us to calculate current-voltage characteristics in the whole range of junction transparency $0<D<1$. However, in the I-V characteristics obtained with this method the subharmonic gap structure is lost because the sideband lattice is washed out (this is illustrated in Fig. 1).

Below we will use dimensionless quantities $E/\Delta, E_n/\Delta \rightarrow E, E_n$. Expanding (the homogeneous) equation (3.2a) from the lattice E_n, $n=odd$ to the continuous axis, $E_n\rightarrow\epsilon$, and keeping the nonlocality of the coefficients (3.3) to first order in eV/Δ, we arrive at the following equation:

$$\left[\left(1-\frac{\omega}{2}\gamma'(\alpha+\coth\gamma)\right)e^{\omega d/d\epsilon}+\left(1-\frac{\omega}{2}\gamma'(\alpha-\coth\gamma)\right)e^{-\omega d/d\epsilon}-2U(\epsilon)+\alpha\omega\gamma'\right]f(\epsilon)=0, \quad (3.4)$$

$$U(\epsilon)=1+(2/D)(\epsilon^2-1).$$

In Eq. (3.4), $\omega=2eV/\Delta$ is the dimensionless Josephson frequency, $\gamma'=d\gamma/d\epsilon$, and the index $\alpha=\pm$ is introduced in order to keep trace of both solutions with $\pm\gamma$, necessary for calculation of the current in Eqs. (2.16), (2.17). Equation (3.4) is valid on the whole axis ϵ except of the point $\epsilon=0$ where the coefficients $A^\pm$ in Eq. (3.3) have a discontinuity in the limit $\omega\rightarrow0$. This results in discontinuity of the function f, which can be taken into account by multiplying the continuous solution $\tilde{f}$ of Eq. (3.4) by a discontinuity factor,

$$f(\epsilon)=e^{i\omega(\pi/2)\theta(\epsilon)}\tilde{f}(\epsilon). \quad (3.5)$$

Equation (3.4) in the classical limit $\omega\rightarrow0$ has a simple physical interpretation: it describes one-dimensional motion of a particle with the dispersion law $\cos\omega\tau$ in the potential

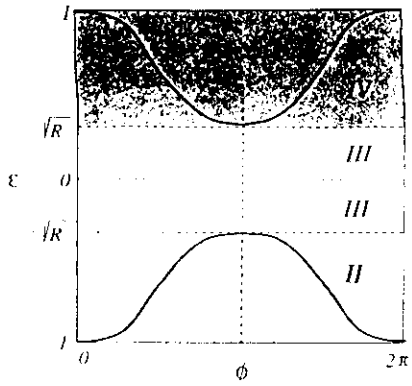

FIG. 3. Energy-phase diagram of static Andreev bound-state bands $\epsilon(\phi)$.

$-U(\epsilon)$, $\cos\omega\tau - U(\epsilon)=0$. This motion corresponds to adiabatic oscillations of the Andreev bound states[28,32,33] in a voltage-biased junction:

$$\epsilon(\phi) = \pm\sqrt{1 - D\sin^2[\phi(\tau)/2]}, \quad \phi(\tau) = \omega\tau, \quad \tau = \Delta t. \tag{3.6}$$

Furthermore, Eq. (3.6) determines classically allowed regions in Eq. (3.4) which coincide with the position of the static Andreev bound bands $\epsilon(\phi)$, $\sqrt{R} < |\epsilon| < 1$, Fig. 3. The energy gap between the Andreev bands, $|\epsilon| < \sqrt{R}$, together with the continuum spectrum, $|\epsilon| > 1$, constitute forbidden regions. Applicability of the quasiclassical approximation requires that the size of each region is much larger than the spacing of the sideband lattice,

$$\min(D, \sqrt{R}) \gg \omega. \tag{3.7}$$

The wave equation (3.4) gives a description of the dynamics of the Andreev bound states in an energy domain which is complementary to the time-domain description developed in Ref. 23; it allows us to treat nonadiabatic effects of Andreev bound-state dynamics. The quasiclassical solution of Eq. (3.4) reads

$$\tilde{f}_{\pm}(\epsilon_0, \epsilon) = \left| \frac{D}{\epsilon^2 - R} \right|^{1/4} e^{\pm S_\alpha(\epsilon_0, \epsilon)}. \tag{3.8}$$

In classically allowed regions (regions *II* and *IV* in Figs. 3 and 4), the quasiclassical exponent S_α has the form

$$S_\alpha(\epsilon_0, \epsilon) = \int_{\epsilon_0}^{\epsilon} d\epsilon' \left(\frac{i}{\omega} \arccos U(\epsilon') + \frac{\alpha}{2\sqrt{\epsilon'^2 - R}} \right),$$

$$\sqrt{R} < |\epsilon| < 1. \tag{3.9a}$$

In the forbidden regions outside the superconducting energy gap (regions *I* and *V*–*VI*), the quasiclassical exponent S_α reads

$$S_\alpha(\epsilon_0, \epsilon) = \int_{\epsilon_0}^{\epsilon} d\epsilon' \left\{ \frac{1}{\omega} \operatorname{arccosh} U(\epsilon') - \frac{\alpha\, \mathrm{sgn}\,\epsilon'}{2\sqrt{\epsilon'^2 - R}} \right\},$$

$$|\epsilon| > 1, \tag{3.9b}$$

while within the Andreev gap (region *III*)

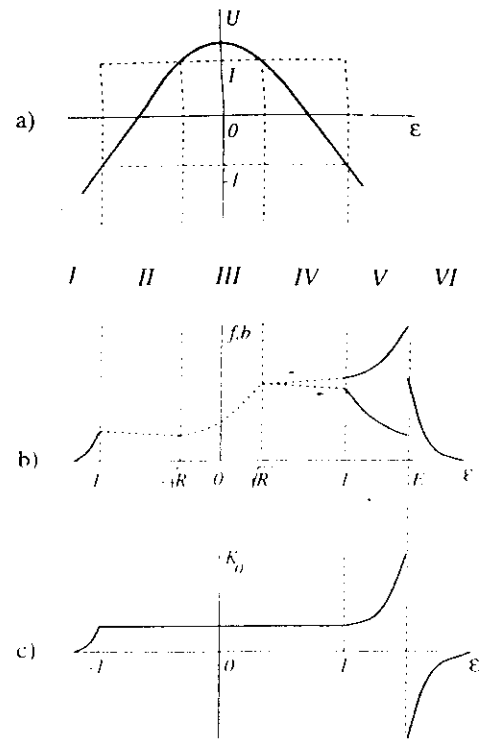

FIG. 4. Scattering state on the energy axis: (a) effective potential; (b) solution of Eq. (3.4): the dotted line represents an envelope of rapidly oscillating wave function; in regions *IV* - *V* the incoming and the reflected waves are shown separately, indicated by arrows; (c) spectral distribution of the dc current, which is constant inside the gap due to compensation of normal (f) and Andreev (b) current channels; this compensation is absent in regions *V*, *VI*.

$$S_\alpha(\epsilon_0, \epsilon) = \int_{\epsilon_0}^{\epsilon} d\epsilon' \left(\frac{1}{\omega} [i\pi - \operatorname{arccosh}|U(\epsilon')|] + \frac{\alpha i}{2\sqrt{R - \epsilon'^2}} \right), \quad |\epsilon| < \sqrt{R}. \tag{3.9c}$$

In Eqs. (3.8), (3.9) only the main branch of the function $\phi(\epsilon)$ in Eq. (3.6) is used, since we are only interested in the values of $\tilde{f}(\epsilon)$ on the lattice $\epsilon = E_n$ where all branches give the same magnitude of $\tilde{f}$.

It is interesting to note the role of small nonadiabatic (proportional to ω) corrections to the coefficients of equation (3.4). These terms contribute to the pre-exponential factors in the quasiclassical solutions and cannot be neglected. Containing an imaginary part, they cause violation of the conservation of the probability current in Eq. (3.4); this leads to specific interference effects in the spectral distribution of the inelastic-scattering amplitudes [see below Eq. (4.6) and following discussion]. Also, they cause suppression of reflection at the edges of the superconducting gap $|\epsilon| = 1$, which are the singular points of the quasiclassical solutions.

Indeed, in the vicinity of the gap edge points $\epsilon = \pm 1$, Eq. (3.4) reduces to

$$\omega^2 f'' - \frac{\omega^2}{2(\epsilon \mp 1)} f' \mp \frac{8}{D}(\epsilon \mp 1) f = 0.$$

the exact solution of which, $f=\exp[\pm(4/3)\sqrt{2/D\omega^2}(\pm\epsilon-1)^{3/2}]$, does not contain any reflected wave. Thus, the matching conditions at the superconducting gap edges are determined by analytic continuation of the exponents S_α in Eqs. (3.9):

$$f_{\pm}^{I}(-1,\epsilon)\to f_{\pm}^{II}(-1,\epsilon), \tag{3.10}$$

$$f_{\pm}^{V}(1,\epsilon)\to f_{\pm}^{IV}(1,\epsilon).$$

In contrast to the superconducting gap edges, the edges of the Andreev gap, $\epsilon=\pm\sqrt{R}$, are true turning points. To derive the matching conditions at these points we first separate out rapid oscillations of the solutions by introducing $\tilde{f}=e^{i\pi\epsilon/\omega}g$. Then Eq. (3.4) reduces to a parabolic cylinder equation in the vicinity of each turning point,

$$\omega^2 g''+\left[\frac{4}{D}(\epsilon^2-R)+\frac{2i\alpha\omega}{\sqrt{D}}\right]g=0. \tag{3.11}$$

If the turning points are well separated, $R\gg D\omega^{1/3}$, Eq. (3.11) further reduces to the Airy equation. Then the standard matching procedure carried out, e.g., at the point $\epsilon=-\sqrt{R}$, yields the relation

$$\begin{pmatrix} C_{+}^{III} \\ C_{-}^{III} \end{pmatrix}=\begin{pmatrix} (1/2)e^{i\pi/4} & (1/2)e^{-i\pi/4+2\pi i(E+\sqrt{R})/\omega} \\ e^{i\pi/4+2\pi i(E+\sqrt{R})/\omega} & e^{i\pi/4} \end{pmatrix}\begin{pmatrix} C_{+}^{II} \\ C_{-}^{II} \end{pmatrix} \tag{3.12}$$

between the coefficients of linear combinations

$$f(\epsilon)=C_{+}f_{+}(\epsilon_0,\epsilon)+C_{-}f_{-}(\epsilon_0,\epsilon) \tag{3.13}$$

in regions III and II (the quasiclassical exponents are here counted from the boundary $\epsilon_0=-\sqrt{R}$). The matching equation (3.12) takes into account exponentially small terms in the asymptotics of the Airy functions in the under-the-barrier region,[34] which is necessary for consistency with the conservation law (2.20). The solutions in regions III and IV are related in a similar way. Combining both matching equations with the solution inside the Andreev gap, $-\sqrt{R}<\epsilon<\sqrt{R}$, we find a direct relation between the coefficients $C_{\pm}$ in Eq. (3.13) in the allowed regions II and IV.

$$\begin{pmatrix} C_{+}^{IV} \\ C_{-}^{IV} \end{pmatrix}=\hat{t}\begin{pmatrix} C_{+}^{II} \\ C_{-}^{II} \end{pmatrix}, \tag{3.14}$$

where transfer matrix $\hat{t}$ has elements

$$t_{12}=t_{21}^{*}=i(e^{\Phi}+e^{-\Phi}/4)e^{-2\pi iE/\omega}, \tag{3.15}$$

$$t_{11}=t_{22}^{*}=(e^{\Phi}-e^{-\Phi}/4)e^{2\pi i\sqrt{R}/\omega},$$

$$\mathrm{Det}\hat{t}=-1,$$

$$\Phi=\frac{1}{\omega}\int_{-\sqrt{R}}^{\sqrt{R}}d\epsilon\,\mathrm{arccosh}|U(\epsilon)|.$$

If the Andreev gap is narrow, $R\ll D\omega^{1/3}$, and the turning points are not well separated, the transfer matrix $\hat{t}$ is found directly from equation (3.11),

$$t_{12}=t_{21}^{*}=ie^{\pi R/\omega-2\pi iE/\omega}, \tag{3.16}$$

$$t_{11}=t_{22}^{*}=\sqrt{R/2\pi\omega}\,\Gamma(iR/\omega)(1-e^{2\pi R/\omega})e^{-\pi R/2\omega}$$

$$\times\exp(-(iR/\omega)[1+\ln(\omega/R)]$$

$$-2\pi i\sqrt{R}/\omega-\pi i/4).$$

where Γ is the Γ function and $\mathrm{Det}\hat{t}=-1$.

The off-diagonal matrix element t_{12} of the transfer matrix $\hat{t}$ has the meaning of inverse amplitude of tunneling through the Andreev gap. The probability of tunneling $W=|t_{12}|^{-2}$ resulting from Eq. (3.15) is

$$W=e^{-2\Phi}=\begin{cases} e^{-\pi\Delta R/eV}, & R\ll 1, \\ e^{(2\Delta/eV)\ln(D/16)}, & D\ll 1. \end{cases} \tag{3.17}$$

In the high transparency limit $R\ll 1$ the result (3.17) coincides with the tunneling probability that follows directly from Eq. (3.16).

Evaluation of the coefficients $C_{\pm}$ in all regions is completed by taking into account the boundary condition at infinity, $f(\pm\infty)=0$, and the source term in Eq. (3.2). Assuming in Eq. (3.2a)

$$f_{-2k-1}=A\lambda^{k}+B\lambda^{-k},\quad f_{2k+1}=C^{VI}\lambda^{-k}, \tag{3.18}$$

for $k=0,1$ with $\lambda=\exp[\,\mathrm{arccosh}U(E)]$, and neglecting the variation of the coefficients with n, we find

$$B=\frac{\xi}{d}(\sqrt{D}+\alpha),\quad C^{VI}-A=\frac{\xi}{d}(\sqrt{D}-\alpha),\ \xi\ll D. \tag{3.19}$$

The explicit form of the coefficients $C_{\pm}$ in all regions for different choices of boundaries ϵ_0 is presented in Table I.

Calculation of the scattering amplitudes b in Eq. (3.2b) is carried out in a similar way. This leads to the equations

$$B=\frac{\alpha\xi r}{d},\quad C_{-}^{VI}=\frac{t_{22}}{t_{12}}Be^{-2S_{-\alpha}(\sqrt{R},\epsilon)}-\frac{\alpha\xi r}{d}. \tag{3.20}$$

The other coefficients in regions $I-VI$ have the same analytical form as the ones in Table. I, the coefficient B being given by Eq. (3.20) and the exponent $S_{-\alpha}$ substituting for S_α.

TABLE I. Reference points ϵ_0 and coefficients $C_\pm$ of linear form in Eq. (3.13) for quasiclassical solutions of wave equation (3.4) for transmitted amplitude f in different regions $I-VI$.

	ϵ_0	C_+	C_-
I	1	$\frac{B}{t_{12}} e^{-2S_a(\sqrt{R},1)-S_a(1,E)}$	0
II	$-\sqrt{R}$	0	$\frac{B}{t_{12}} e^{-S_a(\sqrt{R},E)}$
III	$-\sqrt{R}$	$\frac{B}{2t_{12}} e^{-S_a(\sqrt{R},E)} e^{-\pi/4-2\pi(E+\sqrt{R})/\omega}$	$\frac{B}{t_{12}} e^{-S_a(\sqrt{R},E)} e^{\pi/4}$
IV	$\sqrt{R}$	$Be^{-S_a(\sqrt{R},E)}$	$\frac{t_{22}}{t_{12}} Be^{-S_a(\sqrt{R},E)}$
V	1	$Be^{-S_a(1,E)}$	$\frac{t_{22}}{t_{12}} Be^{-2S_a(\sqrt{R},1)-S_a(1,E)}$
VI	E	0	$\frac{t_{22}}{t_{12}} Be^{-2S_a(\sqrt{R},E)+\frac{\xi}{d}(\sqrt{D}-\alpha)}$

The solutions found above resemble scattering states of a quantum particle propagating along the energy axis through a potential barrier, related to the gap between Andreev bound bands as illustrated in Fig. 4. The amplitude of the incoming wave is determined at the injection point $\epsilon=E$ by the source terms in Eqs. (3.2). Decaying towards the superconducting gap edge, the incoming wave transforms without reflection into a propagating wave within the superconducting gap. Approaching the Andreev gap, it is partially reflected and partially transmitted through the Andreev gap with probability W into the other Andreev band. Then, after approaching the other superconducting gap edge at $\epsilon=-1$, it finally decays outside the superconducting gap. The condition of wave-function decay at infinity plays the role of the outgoing condition in conventional scattering problems determining transmitted and reflected waves. Such a scattering state along the E axis gives a complete description of the spectral distribution of inelastic-scattering amplitudes of the original scattering problem—it therefore provides a basis for calculation of the current through the junction.

IV. TIME-INDEPENDENT CURRENT

In this section we evaluate the time-independent component of the current. This current consists of the sum of incoherent contributions, $N=0$, of all the sidebands in Eq. (2.16). Assuming that the current spectral density K_{nn} varies slowly with sideband index n, we approximate the sum over n with the integral along ϵ,

$$I_0=\frac{e\Delta}{\pi}\int_1^\infty \frac{dE\,E}{\xi}\tanh(E\Delta/2T)\int_{-\infty}^{\infty}\frac{d\epsilon}{\omega}K_0(E,\epsilon), \quad (4.1)$$

$$K_0(E,\epsilon)=\cosh[\mathrm{Re}\,\gamma(\epsilon)]\{[|f(E,\epsilon)|^2-|b(E,\epsilon)|^2]^{-1}-(\gamma\to-\gamma)\}.$$

We will distinguish three components in the averaged current: single-particle current of the real excitations I_+ (region I, $\epsilon>1$), pair current of the Andreev bound states I_Δ (regions $II-IV$, $-1<\epsilon<1$), and current of the ground-state modes I_- (regions $V-VI$, $\epsilon<1$),

$$I_0=I_++I_\Delta+I_-. \quad (4.2)$$

According to the conservation law Eq. (2.20), the current spectral density K_0 does not depend on ϵ within the superconducting gap, $K_0(\epsilon)=\mathrm{const}$ (Fig. 4). K_0 is easily evaluated at superconducting gap edge $\epsilon=-1$,

$$K_0(E,|\epsilon|<1)=K_0(E,-1)=\frac{4\xi^2W}{\sqrt{D}}e^{-2S(1,E)}. \quad (4.3)$$

Thus the current spectral density is exponentially small *everywhere within the superconducting gap* if $R>\omega$, i.e., for sufficiently low voltage [cf. Eq. (3.17)]. Multiplying equation (4.3) by 2, the size of the gap region, and performing integration over energy E, we get

$$I_\Delta=\frac{2e\Delta W}{\pi}\tanh(\Delta/2T). \quad (4.4)$$

This current gives the main contribution to the time-independent current at zero temperature. We notice, that the voltage dependence enters Eq. (4.4) only through the tunneling probability W, while the large pre-exponential factor ω^{-1} in Eq. (4.1) related to the large number of Andreev bound states is compensated for by a small phase volume of relevant scattering states, $E-1\sim(D\omega^2)^{1/3}$. In accordance with the voltage dependence of W in Eq. (3.17), the current in Eq. (4.4) undergoes crossover from the contact to the tunnel regime at $eV\sim\pi R\Delta$ (cf. Refs. 23,25), as shown in Fig. 5.

The current spectral density K_0 rapidly decays with departure from the energy gap into region I and is concentrated

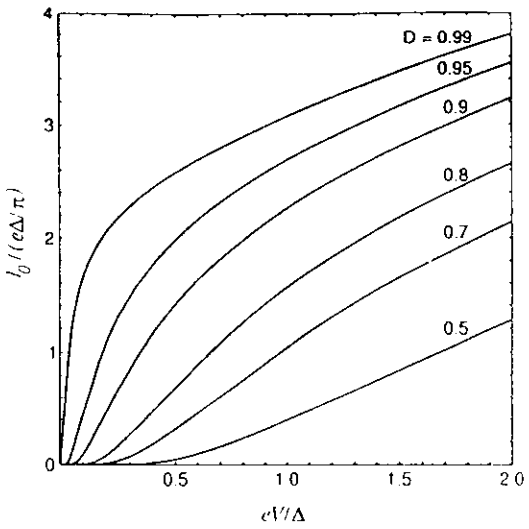

FIG. 5. Current I_0 vs applied voltage at different junction transparencies.

in a narrow interval $\epsilon+1\sim(D\omega^2)^{1/3}$. This yields a small magnitude of the current of real excitations $I_<$ in comparison with the pair current I_Δ,

$$I_<=\frac{e\Delta W}{2\pi}a(D\omega^2)^{1/3}\tanh(\Delta/2T), \tag{4.5}$$

$$a=\Gamma(2/3)/6^{1/3}=0.742.$$

Let us now discuss the currents in regions $V-VI$:

$$K_0^V(E,\epsilon)=\frac{4\xi^2}{\sqrt{D}}e^{-2S(1,E)}(e^{2S(1,\epsilon)}-|Q|^2e^{-2S(1,\epsilon)}) \tag{4.6a}$$

$$K_0^{VI}(E,\epsilon)=-\frac{4\xi^2}{\sqrt{D}}e^{-2S(1,\epsilon)}(e^{2S(1,E)}+|Q|^2e^{-2S(1,E)} -2\sqrt{R}ReQ). \tag{4.6b}$$

The quantity

$$Q=\frac{t_{22}}{t_{12}}\exp\left(-\frac{2i}{\omega}\int_{\sqrt{R}}^{1}\arccos V dE\right), \tag{4.7}$$

in Eqs. (4.6) has the meaning of the amplitude of reflection from the superconducting gap. The ratio

$$t_{22}/t_{12}=\sqrt{1-W}e^{-i\pi/2+(2i\pi/\omega)(E-\sqrt{R})} \tag{4.8}$$

is the reflection amplitude caused by the Andreev gap, and the oscillating factor in Eq. (4.7) contains the additional phase gained during propagation through the region IV. Thus the first terms in the brackets in Eqs. (4.6) correspond to the currents of incoming and reflected waves while the third term in Eq. (4.6b) is the interference current.

In contrast to regions $I-IV$, the current spectral densities K_0^V and K_0^{VI} are not exponentially small (Fig. 4). However, at zero temperature one should expect very precise cancellation of these currents since the imbalance effect is only produced by the creation of a tiny amount of real excitations. Indeed,

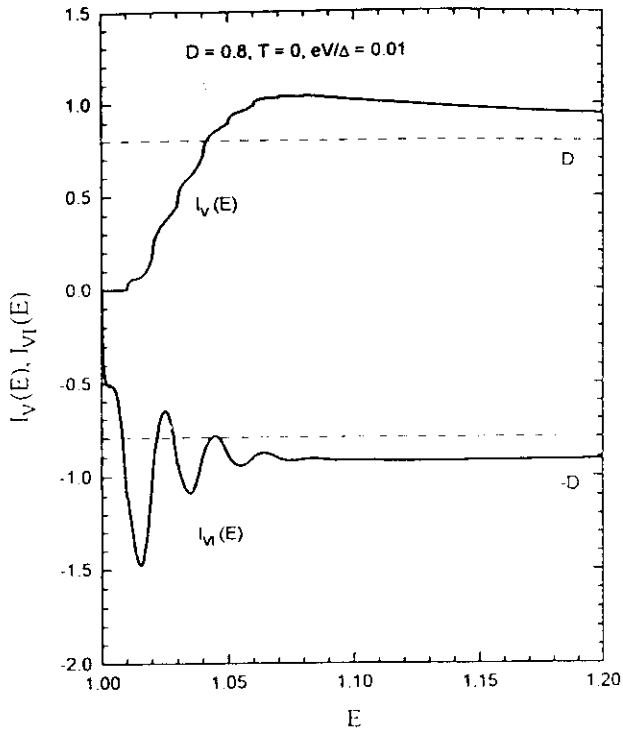

FIG. 6. Currents in regions $V-VI$ calculated from the exact recurrences (2.10); currents $I_V(E)$ and $I_{VI}(E)$ represent current densities K_0^V and K_0^{VI} from Eq. (4.6) respectively, integrated over ϵ. The current I_{VI} reveals pronounced oscillations vs E reflecting the interference term in Eq. (4.6b), while the interference effect in I_V is much smaller. The asymptotics at large E correspond to the current spectral density in the normal junctions.

the dissipative current I_0 determines the rate $\dot{\mathcal{E}}$ of energy transfer from the external source to the electron system: $\dot{\mathcal{E}}=VI_0$. This energy is expended for creation of real excitations; it consists of the product of energy 2Δ lost to single excitation, the tunneling probability W, and the frequency of attempts eV: $\dot{\mathcal{E}}\sim 2\Delta WeV$. This rough estimate yields $I_0\sim I_\Delta$. Direct calculation of noninterference currents in Eqs. (4.6) supports the above conclusion: the currents of regions $V-VI$ compensate each other with exponential accuracy after integration over energy E, giving the result

$$I_>=\frac{e\Delta W}{2\pi}a(D\omega^2)^{1/3}. \tag{4.9}$$

This coincides with the current of real excitations $I_<$, Eq. (4.5). At the same time, the interference current is not canceled but yields a residual oscillating current which is not exponentially small. This result apparently contradicts the above arguments (exponentially small I_0) and also the result of exact numerical calculation of the subharmonic gap structure in Fig. 1, which does not show any background current in the limit of low voltage.

The correct behavior is revealed by detailed numerical investigation of the currents in regions $V-VI$ carried out on the basis of the exact recurrences in Eq. (2.10). In Fig. 6, the currents $I_V(E)$ and $I_{VI}(E)$ show the integral contribution of the regions V and VI [the current densities in Eqs. (4.6)

integrated over ϵ]. The current in region *VI* shows pronounced interference oscillations similar to our analytical result in Eq. (4.6b). The current in region *V* also possesses an oscillating component but with much smaller amplitude. This oscillating component is not present in Eq. (4.6a) because of its small magnitude ($\sim\omega$), which exceeds the accuracy of the quasiclassical approximation. The full-scale rapid oscillations of current in region *VI* are reduced after integration over energy and they are perfectly compensated for by the current from region *V*.

At finite temperature the current compensation is lifted due to the energy-dependent Fermi factor in Eq. (4.1), which yields a current of thermal excitations that is not exponentially small (with respect to eV). The smooth part of this current, resulting from noninterfering terms in Eqs. (4.6), has the form

$$I_>(T)=\frac{2e^2V}{\pi}\sqrt{\frac{\pi\Delta D}{2T}}e^{-\Delta/T},\quad T/\Delta\ll D. \tag{4.10}$$

In the opposite limit the current of thermal excitations is

$$I_>(T)=\frac{e^2DV}{4\pi}\frac{\Delta}{T}\left(\frac{\pi}{2}-1\right)\cosh^{-2}\frac{\Delta}{2T},\quad D\ll T/\Delta\ll 1. \tag{4.11}$$

The result of numerical evaluation of the smooth current component is plotted in Fig. 7 with dashed lines. The solid lines show the exact current of thermal excitations which manifests pronounced oscillating features. Although the accuracy of the quasiclassical approximation is not sufficient for analytical evaluation of the amplitude of current oscillations $\delta I_{\rm osc}$, as previously explained, the oscillation period Π: $\delta I_{\rm osc}[(\Delta/eV)+\Pi]=\delta I_{\rm osc}(\Delta/eV)$, can easily be evaluated from Eqs. (4.7), (4.8). Since integration over energy selects the energy $E=1$, the oscillation period is

$$\Pi=\frac{\pi}{\int_0^{\pi}(\pi-\phi)dE(\phi)}. \tag{4.12}$$

where $E(\phi)$ is the static Andreev bound-state spectrum, Eq. (3.6). For low transparency, Eq. (4.12) reads

$$\Pi\approx\frac{8}{D},\quad D\ll 1.$$

In Fig. 8, the junction conductance $G=I/V$ is plotted as a function of inverse voltage. The oscillations are clearly periodic and the period does not depend on temperature. The numerical evaluation of the period is in nice agreement with Eq. (4.12).

V. TIME-DEPENDENT CURRENT

Proceeding to calculation of the time-dependent ($N\neq 0$) part of the current in Eq. (2.16), we note that the quasiclassical approximation only allows us to investigate low-frequency current harmonics, $N\omega\ll 1$. Within such an approximation one can neglect the difference between indices of coefficients of bilinear form in Eq. (2.17).

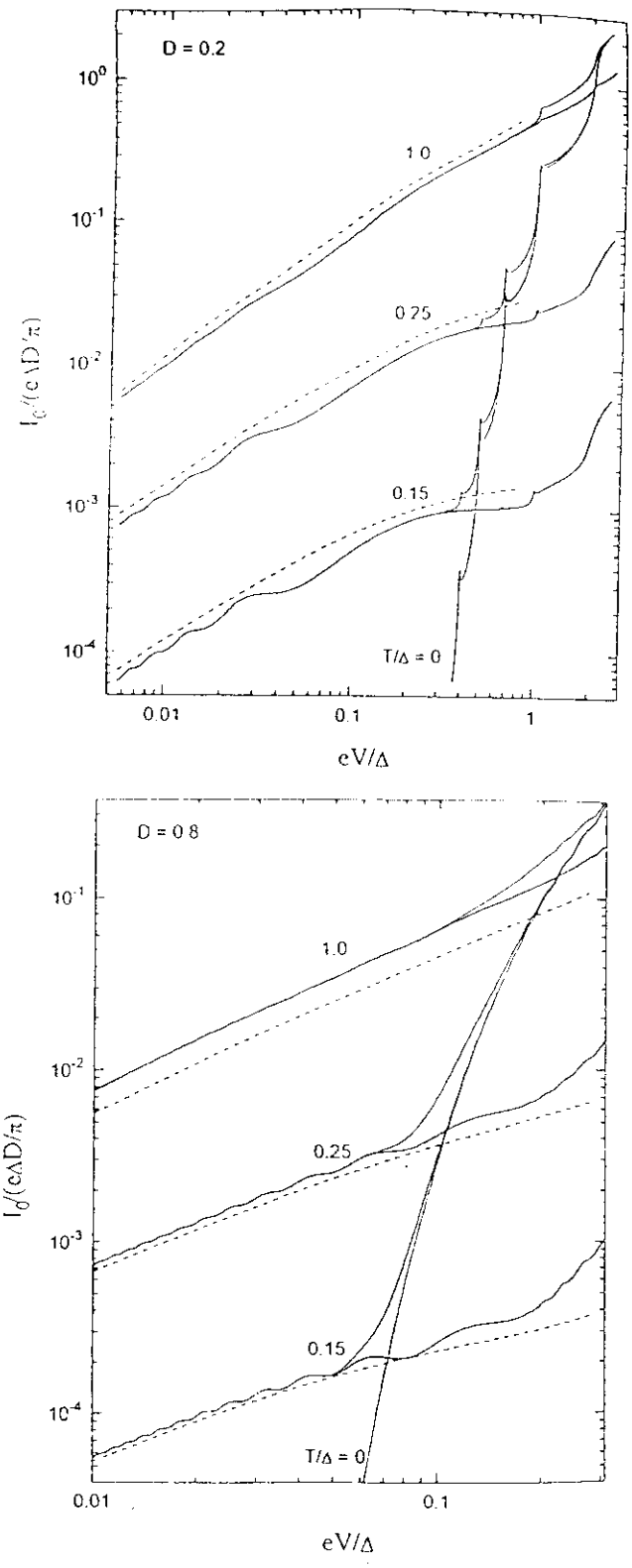

FIG. 7. *I-V* characteristics of junctions with transparencies D = 0.2 (upper) and D = 0.8 (lower) at different temperatures [normalized by $\Delta(T)$]. Bold lines represent exact numerical results for the current of thermal excitations (regions *V* - *VI*); dashed lines are the results of quasiclassical theory without inclusion of the interference term; thin lines show the total dc current, coinciding with the thermal excitation current at low voltage.

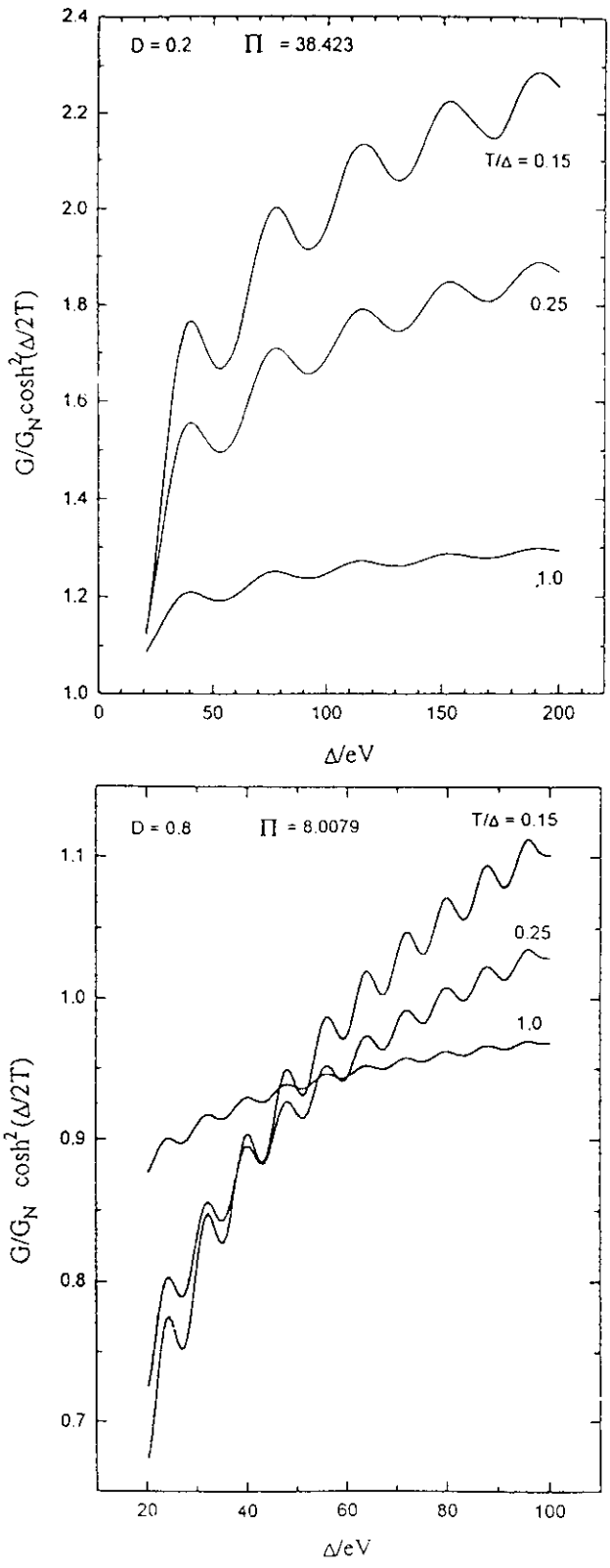

FIG. 8. Oscillations of the normalized junction conductance $G(T)=I(T)/V$ vs inverse voltage at different temperatures in junctions with transparencies $D = 0.2$ (upper) and $D = 0.8$ (lower); $G_N = e^2 D/\pi$ is the conductance of the normal junction. The period of oscillations is given by Eq. (4.12).

$$I_{ac}=\frac{e\Delta}{\pi}\sum_{N=1}^{\infty}\int_1^{\infty}\frac{dEE}{\xi}\tanh(E\Delta/2T)\times\int_{-\infty}^{\infty}\frac{d\epsilon}{\omega}\,2\,\mathrm{Re}[e^{iN\omega\tau}K_N(E,\epsilon)]. \tag{5.1}$$

$$K_N(E,\epsilon)=\cosh[\,\mathrm{Re}\,\gamma(\epsilon)]\{[f^*(\epsilon+N\omega)f(\epsilon)-b^*(\epsilon+N\omega)b(\epsilon)]-(\gamma\to-\gamma)\}.$$

Furthermore, when calculating products of scattering amplitudes in Eq. (5.1), we will assume coinciding arguments in the pre-exponential factors in Eq. (3.8) and expand quasiclassical exponents: $S(\epsilon+N\omega)\approx S(\epsilon)+S'N\omega$. The main contribution to the ac current at all temperatures results from regions II and IV—classically allowed regions for Andreev bound-state oscillations. The current spectral density K_N^{II} differs from the static Eq. (4.3) containing the additional exponential factor $\exp(S'N\omega)\approx\exp[iN\phi(\epsilon)]$:

$$K_N^{II}(E,\epsilon)=\frac{4\xi^2 W}{\sqrt{D}}e^{-2S(1,E)}e^{iN\phi(\epsilon)}, \tag{5.2}$$

where $\phi(\epsilon)$ is given by Eq. (3.6). The current spectral density in region IV only consists of incoherent contributions of incoming waves and waves reflected from the Andreev gap,

$$K_N^{IV}(E,\epsilon)=\frac{4\xi^2}{\sqrt{D}}e^{-2S(1,E)}(e^{-iN\phi(\epsilon)}-|Q|^2e^{iN\phi(\epsilon)}) \tag{5.3}$$

(the interference current vanishes in the quasiclassical approximation). Combination of Eqs. (5.2), (5.3), and (5.1) yields the ac current,

$$I_{ac}^{II+IV}=\frac{e\Delta D}{2}\tanh\frac{\Delta}{2T}\left[(1-W)\frac{\sin\omega\tau}{\sqrt{1-D\sin^2(\omega\tau/2)}}+W\left(\frac{|\sin\omega\tau|}{\sqrt{1-D\sin^2(\omega\tau/2)}}-\frac{4(1-\sqrt{R})}{\pi D}\right)\mathrm{sgn}V\right], \tag{5.4}$$

which consists both of sine and cosine components (odd and even with respect to time reversal) and undergoes crossover from cosine-like behavior in the contact limit $D=1$ ($W=1$) to sine-like behavior in the tunnel limit $D\ll 1$ ($W\ll 1$). A similar crossover occurs with decreasing voltage when $R\ll 1$: from cosine-like behavior at comparatively large voltage, $eV\gg R\Delta$, to sine-like behavior at low voltage $eV\ll R\Delta$. We note that the instant current in Eq. (5.4) in the limit $V\to 0$ does not approach the static Josephson current, having different temperature dependence. The dc Josephson current possesses a temperature dependence $\tanh(E(\phi)\Delta/2T)$ with $E(\phi)$ given by Eq. (3.6), which reflects the equilibrium population of the static Andreev bound states. In contrast, the temperature factor in Eq. (5.4) reflects the nonequilibrium population of oscillating Andreev states through the Fermi filling factor at the gap edge $E=1$. Such a difference persists unless the period of Josephson oscillations exceeds the inelastic relaxation time.[7,24]

The last, time-independent, term in Eq. (5.4) is equal to the zeroth harmonic of the current of regions II,IV, and

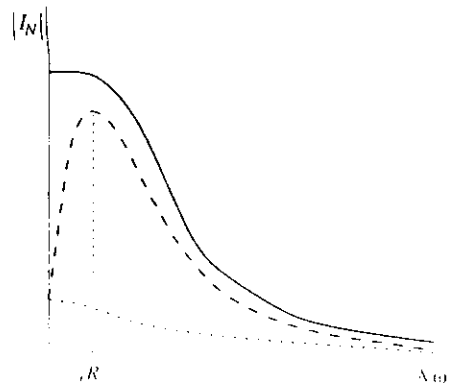

FIG. 9. Spectral distribution of the cosine harmonics of the ac Josephson current. The solid line is the fully transparent junction ($R=0$); dotted line is the junction with finite reflectivity ($R>\omega$), contribution of Andreev bound states; dashed line is the junction with finite reflectivity ($R\gg\omega$), total cosine current with account of contribution of the Andreev gap.

therefore represents the time-averaged magnitude of the total ac current of the oscillating quasistatic Andreev states. It was pointed out in Ref. 23 that in fully transparent junctions, $R=0$, the dc current is entirely produced by oscillating Andreev states. In junctions with finite reflectivity, $R>0$, according to Eq. (5.4) only part of dc pair current, Eq. (4.4), results from oscillating Andreev states—the remaining part is contributed by nonadiabatic states within the Andreev gap (region *III*).

The conclusion drawn above about the exponentially small magnitude of the cosine current in the tunnel regime concerns, rigorously speaking, only the low-frequency part of the ac current. The suppression of the low-frequency current is caused by the conservation law in Eq. (2.20), which is nearly fulfilled in this frequency region and which establishes approximate balance of the normal and Andreev currents. On the other hand, one has to expect that high-frequency harmonics are not suppressed: harmonics in the region $N\omega\gg\sqrt{R}$ should not be sensitive to the presence of a gap in the static Andreev spectrum and must approximately have the same magnitude as the cosine harmonics in fully transparent junctions, $R=0$. Such arguments lead to the spectrum of the cosine ac current sketched in Fig. 9: the amplitudes of the harmonics, being exponentially small at small N, rapidly grow with N and after approaching a maximum at $N\omega\sim\sqrt{R}$ decay with a power law, similarly to the spectrum of the transparent junction. The nonadiabatic effect of exponential growth of the harmonic amplitudes at low frequency is provided by the contribution of the forbidden region *III*.

The contribution of forbidden regions to the ac current is always restricted to the cosine component,

$$I_{ac}=\sum_{N=1}^{\infty} I_N\cos(N\omega\tau). \tag{5.5}$$

The current contribution of region *III*

$$I_N^{III}=\frac{4e\Delta W}{\pi}\tanh\frac{\Delta}{2T}(-1)^N\int_0^{\sqrt{R}}d\epsilon\cosh(N\,\mathrm{arccosh}|U(\epsilon)|) \tag{5.6}$$

results from the interference terms $f_+^*(\epsilon+N\omega)f_-(\epsilon)$, and other similar terms, which combine growing and decaying elementary solutions. The first harmonics in Eq. (5.6) have the same order of magnitude as the cosine current of oscillating Andreev states in Eq. (5.4). The harmonic amplitudes exponentially grow with N,

$$I_N^{III}=\frac{4e\Delta W}{\pi}\tanh\frac{\Delta}{2T}(-1)^N\left(\frac{\pi\sqrt{R}}{N}\right)^{1/2}$$
$$\times\exp(N\,\mathrm{arccosh}(1+2R/D)),\quad N\gg 1,$$

until $N\omega$ exceeds the size of region *III*, $N_{\max}\sim\sqrt{R}/\omega$.

The spectral density of the ac current in region *I* rapidly decays with departure from the superconducting gap edge, similarly to the dc current. Therefore, its contribution is small with respect to the cosine current of the Andreev states,

$$I_{N\omega\ll\Delta}=\frac{e\Delta W}{\pi}(D\omega^2)^{1/3}a_N\tanh\frac{\Delta}{2T}, \tag{5.7}$$

$$a_N=\int_0^{\infty}dx\exp\left\{-\frac{2}{3}x^{3/2}-\frac{2}{3}(x+2N/N_0)^{3/2}\right\},$$

$$N_0=(D/\omega)^{1/3}.$$

The currents in regions *V* and *VI* nearly compensate each other at zero temperature, yielding a total current coinciding with the contribution of region *I*, $I_{N\gg 1}=I_{N\ll 1}$. At nonzero temperature the current compensation is lifted, which leads to an ac current of thermal excitations. The smooth, noninterference component of this current,

$$I_{N\ll 1}(T)\simeq\frac{4e^2\Delta}{\pi}e^{-\Delta/T}\sqrt{D}\int_0^{\infty}\frac{dx}{x^2}(1-e^{-2Tx^2/\Delta})$$
$$\times\exp(-2N\sqrt{D}x),\ T/\Delta\ll D,\quad N\ll N_0, \tag{5.8}$$

decreases with harmonic number N as N^{-1}. At $N\gg N_0$ the current harmonics decay exponentially.

We conclude this section with a remark about the sign of the cosine current (see the discussion in Ref. 35). Although the signs of all harmonics in Eq. (5.8) are positive, the sign of the total cosine current may be negative due to competition with the cosine current of the Andreev bound states in Eqs. (5.4) and (5.6). In particular, the contribution by the Andreev bound states to the first cosine harmonic is negative.

VI. CONCLUSION

In conclusion, we have calculated the dc current and the ac Josephson current in quantum superconducting junctions at low applied voltage $eV\ll\Delta$ in the whole range of junction transparency $0<D<1$. The global structure of multiple Andreev scattering and the distribution of currents among inelastic-scattering channels is described in terms of the wave function of an effective quasiclassical particle propagating along the energy axis.

The main physical characteristic, which determines the properties of low-biased junctions with intermediate transparency, is the energy gap in the static Andreev bound-state spectrum. Opening of the Andreev gap yields exponential

uppression of the dc current, and determines the crossover rom the contact to the tunnel regime of both the dc current nd the ac Josephson current as functions of junction trans-arency and applied voltage. Quasiparticle reflection from he edges of the Andreev gap causes mesoscopic phenomena nanifested in oscillating features on current-voltage charac-eristics at finite temperature.

At zero temperature, the pair current always gives the nain contribution to the dc current and is homogeneously listributed within the superconducting energy gap. In the unnel regime $eV \ll R\Delta$, the suppression of the low-requency cosine harmonics of the ac current is lifted at igher frequency: the amplitudes of the cosine harmonics row exponentially with the harmonic number N, and chieve at $NeV \sim \sqrt{R}\Delta$ a magnitude of the order of the non-uppressed current in a pure constriction.

The present investigation has been concerned with junc-ons whose scattering properties in the normal state do not epend on energy, which is true for all kinds of weak links ith lengths shorter than the coherence length. However, the ethod can be extended to long superconductor–normal-metal-superconductor junctions, junctions with resonance tunnel barriers, and other structures where electron-hole dephasing effects are important. It has been shown in Ref. 36 that the electron-hole dephasing gives rise to modification of the spectral equation (3.6) to the form $\cos\phi = F[r(E), d(E)]$, where F is a universal function of the electron-scattering amplitudes of the normal part of the junction. Therefore, although the shape of the effective potential in the energy-domain wave equation (3.4) is specifically modified for each particular junction, the whole scenario remains unchanged.

ACKNOWLEDGMENTS

This work has been supported by the Swedish National Science Research Council (NFR), the Swedish National Board for Technical and Industrial Development (NUTEK), and the Swedish Royal Academy of Sciences (KVA). Part of the work has been supported by Grant No. INTAS-94-3861 and by the Ukrainian State Foundation for Fundamental Research, Grant No. 2.4/136.

T.M. Klapwijk, G.E. Blonder, and M. Tinkham, Physica B+C **109-110**, 1657 (1982).
M. Octavio, M. Tinkham, G.E. Blonder, and T.M. Klapwijk, Phys. Rev. B **27**, 6739 (1983).
R. Kümmel and W. Senftinger, Z. Phys. B **59**, 275 (1985).
G.B. Arnold, J. Low Temp. Phys. **68**, 1 (1987).
K. Flensberg, J. Bindslev Hansen, and M. Octavio, Phys. Rev. B **38**, 8707 (1988).
R. Kümmel, U. Gunsenheimer, and R. Nicolsky, Phys. Rev. B **42**, 3992 (1990).
U. Gunsenheimer and A.D. Zaikin, Phys. Rev. B **50**, 6317 (1994).
N.R. Werthamer, Phys. Rev. **147**, 255 (1966).
J.R. Schrieffer and J.W. Wilkins, Phys. Rev. Lett. **10**, 17 (1963); J.W. Wilkins, in *Tunneling Phenomena in Solids*, edited by E. Burstein and S. Lundquist (Plenum, New York, 1969) p. 333.
B.N. Taylor and E. Burstein, Phys. Rev. Lett. **10**, 14 (1963).
J.M. Rowell, Rev. Mod. Phys. **36**, 215 (1963).
C.L. Foden, R. Rando, A. van Dordrecht, A. Peacock, J. Lumley, and C. Pereira, Phys. Rev. B **47**, 3316 (1993).
R. Cristiano, L. Frunzio, R. Monaco, C. Nappi, and S. Pagano, Phys. Rev. B **49**, 429 (1994).
A.W. Kleinsasser, R.E. Miller, W.H. Mallison, and G.B. Arnold, Phys. Rev. Lett. **72**, 1738 (1994).
E.N. Bratus', V.S. Shumeiko, and G. Wendin, Phys. Rev. Lett. **74**, 2110 (1995).
N. van der Post, E.T. Peters, I.K. Yanson, and J.M. van Ruitenbeek, Phys. Rev. Lett. **73**, 2611 (1994).
E. Scheer, P. Joyez, M.H. Devoret, D. Esteve, and C. Urbina (unpublished).
H. Takayanagi, T. Akazaki, and J. Nitta, Phys. Rev. Lett. **75**, 3533 (1995).
R. Landauer, IBM J. Res. Dev. **1**, 223 (1957).
Y. Imry, *Directions in Condensed Matter Physics* (World Scientific, Singapore, 1986), p. 102.
V.S. Shumeiko, E.N. Bratus', and G. Wendin, Low Temp. Phys. **23**, 249 (1997).
N. van der Post (private communication).
D. Averin and A. Bardas, Phys. Rev. Lett. **75**, 1831 (1995).
J.C. Cuevas, A. Martin-Rodero, and A. Levy Yeyati, Phys. Rev. B **54**, 7366 (1996).
E.N. Bratus', V.S. Shumeiko, E.V. Bezuglyi, and G. Wendin, Low Temp. Phys. **22**, 474 (1996).
L.I. Glazman, G.B. Lesovik, D.E. Khmel'nitskii, and R.I. Shekhter, Pis'ma Zh. Éksp. Teor. Fiz. **48**, 218 (1988) [JETP Lett. **48**, 238 (1988)].
P.G. de Gennes, *Superconductivity of Metals and Alloys* (Addison-Wesley, New York, 1989).
V.S. Shumeiko, G. Wendin, and E.N. Bratus', Phys. Rev. B **48**, 13 129 (1993).
I.O. Kulik and A. N. Omel'yanchuk, Fiz. Nisk. Temp. **3**, 945 (1977); **4**, 296 (1978) [Sov. J. Low Temp. Phys. **3**, 459 (1977); **4**, 142 (1978)].
I.O. Kulik, R.I. Shekhter, and A.N. Omel'yanchouk, Solid State Commun. **23**, 301 (1977).
V.P. Galaiko, Zh. Éksp. Teor. Fiz. **61**, 382 (1971) [Sov. Phys. JETP **34**, 203 (1972)].
S.V. Kuplevakhskii and I.I. Fal'ko, Fiz. Nizk. Temp. **17**, 961 (1991) [Sov. J. Low Temp. Phys. **17**, 501 (1991)].
A. Furusaki and M. Tsukada, Physica B **165-166**, 967 (1990).
M. Abramovits and I.A. Stegun, *Handbook of Mathematical Functions*, Appl. Math. Series 55 (National Bureau of Standards, 1968).
A. Barone and G. Paterno, *Physics and Applications of the Josephson Effect* (Wiley, New York, 1982).
G. Wendin and V.S. Shumeiko, Superlattices Microstruct. **20**, 569 (1996).